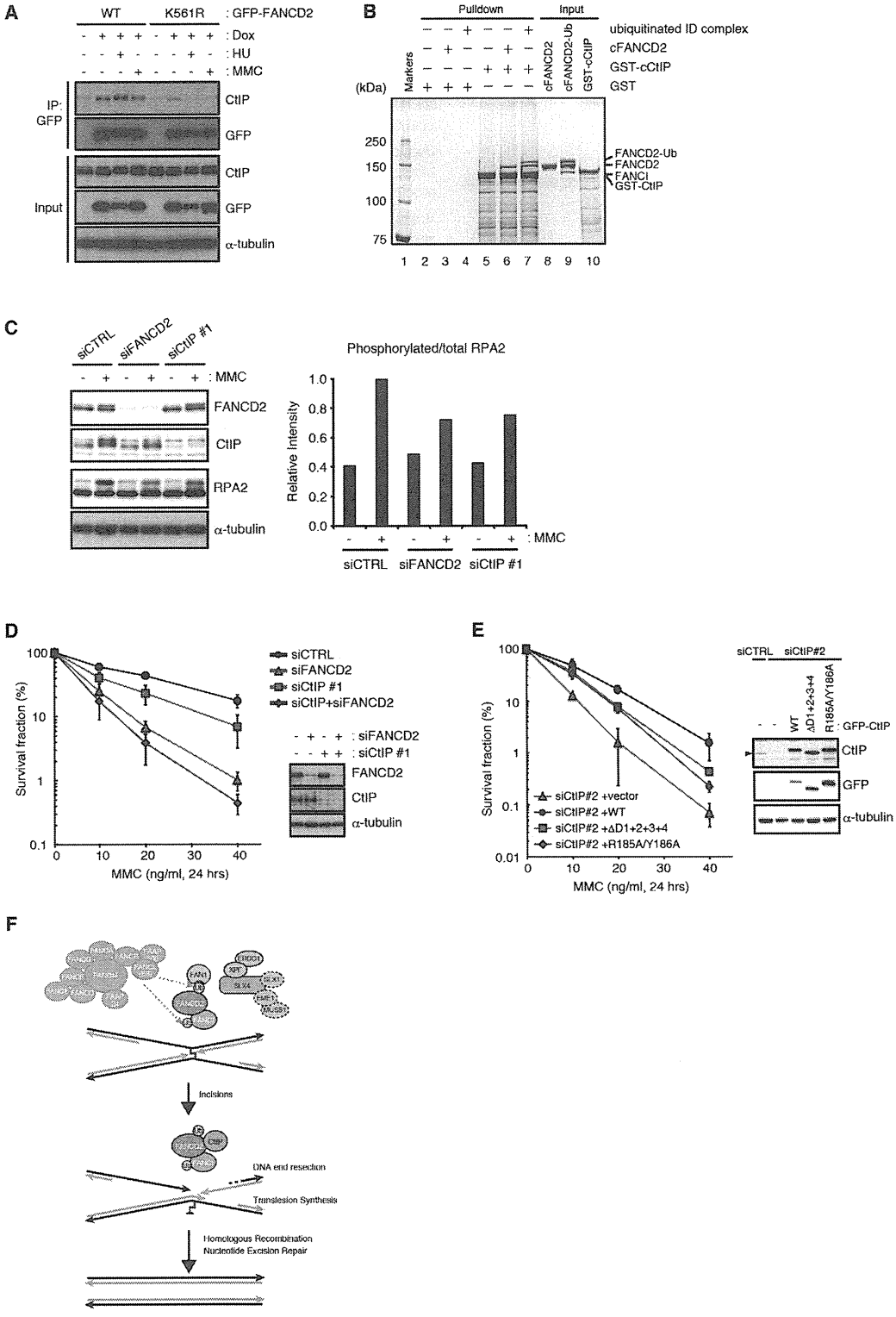

(legend on next page)

were analyzed in each experiment. The in situ PLA was carried out using specific antibodies and a DuoLink in situ PLA kit (Olink Bioscience).

Mammalian Two-Hybrid Analysis

Mammalian two-hybrid assays were carried out as described previously (Pace et al., 2002).

Clonogenic survival assay

Cells were treated with MMC for 24 hr, washed with PBS, and then plated on six-well plates and incubated for 10–14 days.

SUPPLEMENTAL INFORMATION

Supplemental Information includes Supplemental Experimental Procedures and four figures and can be found with this article online at http://dx.doi.org/10.1016/j.celrep.2014.04.005.

AUTHOR CONTRIBUTIONS

A.I. purified the FANCD2 complex with J.T. and T. Ikura; M. Taoka and T. Isobe performed mass spectrometry; K. Sato and H.K. purified proteins and performed in vitro reactions; J.U. performed the rest of the experiments with M.I.; W.S. and K. Sugasawa provided unpublished cell lines; and M. Takata wrote the paper with J.U., K. Sato, and H.K.

ACKNOWLEDGMENTS

We would like to thank Dr. James Hejna (Kyoto University) for critical reading and English editing of the manuscript; Drs. Toshiyasu Taniguchi, Takayuki Yamashita, John Rouse, Richard Mulligan, Matthias Gstaiger, Atsushi Shibata, Penny Jeggo, Maria Jasin, and Agata Smogorzewska for reagents; Dr. Alex Sartori for sharing unpublished data; Ms. Sumiyo Ariga and Chinatsu Ohki for expert technical assistance; and Ms. Seiko Arai for secretarial assistance. This work was supported in part by grants-in aid from the Ministry of Education, Science, Sports, and Culture of Japan (JSPS KAKENHI grant number 21390094 and MEXT KAKENHI grant number 23114010).

Received: August 31, 2013
Revised: March 10, 2014
Accepted: April 4, 2014
Published: May 1, 2014

REFERENCES

Auerbach, A.D. (2009). Fanconi anemia and its diagnosis. Mutat. Res. *668*, 4–10.

Bogliolo, M., Schuster, B., Stoepker, C., Derkunt, B., Su, Y., Raams, A., Trujillo, J.P., Minguillón, J., Ramírez, M.J., Pujol, R., et al. (2013). Mutations in ERCC4, encoding the DNA-repair endonuclease XPF, cause Fanconi anemia. Am. J. Hum. Genet. *92*, 800–806.

Bunting, S.F., Callén, E., Kozak, M.L., Kim, J.M., Wong, N., López-Contreras, A.J., Ludwig, T., Baer, R., Faryabi, R.B., Malhowski, A., et al. (2012). BRCA1 functions independently of homologous recombination in DNA interstrand crosslink repair. Mol. Cell *46*, 125–135.

Chapman, J.R., Taylor, M.R.G., and Boulton, S.J. (2012). Playing the end game: DNA double-strand break repair pathway choice. Mol. Cell *47*, 497–510.

Dubin, M.J., Stokes, P.H., Sum, E.Y.M., Williams, R.S., Valova, V.A., Robinson, P.J., Lindeman, G.J., Glover, J.N.M., Visvader, J.E., and Matthews, J.M. (2004). Dimerization of CtIP, a BRCA1- and CtBP-interacting protein, is mediated by an N-terminal coiled-coil motif. J. Biol. Chem. *279*, 26932–26938.

Duquette, M.L., Zhu, Q., Taylor, E.R., Tsay, A.J., Shi, L.Z., Berns, M.W., and McGowan, C.H. (2012). CtIP is required to initiate replication-dependent interstrand crosslink repair. PLoS Genet. *8*, e1003050.

Hofmann, K. (2009). Ubiquitin-binding domains and their role in the DNA damage response. DNA Repair (Amst.) *8*, 544–556.

Huertas, P. (2010). DNA resection in eukaryotes: deciding how to fix the break. Nat. Struct. Mol. Biol. *17*, 11–16.

Ikura, T., Ogryzko, V.V., Grigoriev, M., Groisman, R., Wang, J., Horikoshi, M., Scully, R., Qin, J., and Nakatani, Y. (2000). Involvement of the TIP60 histone acetylase complex in DNA repair and apoptosis. Cell *102*, 463–473.

Karanja, K.K., Cox, S.W., Duxin, J.P., Stewart, S.A., and Campbell, J.L. (2012). DNA2 and EXO1 in replication-coupled, homology-directed repair and in the interplay between HDR and the FA/BRCA network. Cell Cycle *11*, 3983–3996.

Kim, H., and D'Andrea, A.D. (2012). Regulation of DNA cross-link repair by the Fanconi anemia/BRCA pathway. Genes Dev. *26*, 1393–1408.

Kim, J.M., Kee, Y., Gurtan, A., and D'Andrea, A.D. (2008). Cell cycle-dependent chromatin loading of the Fanconi anemia core complex by FANCM/FAAP24. Blood *111*, 5215–5222.

Kim, Y., Lach, F.P., Desetty, R., Hanenberg, H., Auerbach, A.D., and Smogorzewska, A. (2011). Mutations of the SLX4 gene in Fanconi anemia. Nat. Genet. *43*, 142–146.

Kottemann, M.C., and Smogorzewska, A. (2013). Fanconi anaemia and the repair of Watson and Crick DNA crosslinks. Nature *493*, 356–363.

Murina, O., von Aesch, C., Karakus, U., Ferretti, L.P., Bolck, H.A., Hänggi, K., and Sartori, A.A. (2014). FANCD2 and CtIP Cooperate in the Repair of DNA Interstrand Crosslinks. Cell Rep. *7*, this issue, 1030–1038, this issue.

Pace, P., Johnson, M., Tan, W.M., Mosedale, G., Sng, C., Hoatlin, M., de Winter, J., Joenje, H., Gergely, F., and Patel, K.J. (2002). FANCE: the link between Fanconi anaemia complex assembly and activity. EMBO J. *21*, 3414–3423.

Raynard, S., Niu, H., and Sung, P. (2008). DNA double-strand break processing: the beginning of the end. Genes Dev. *22*, 2903–2907.

Sartori, A.A., Lukas, C., Coates, J., Mistrik, M., Fu, S., Bartek, J., Baer, R., Lukas, J., and Jackson, S.P. (2007). Human CtIP promotes DNA end resection. Nature *450*, 509–514.

Sato, K., Ishiai, M., Toda, K., Furukoshi, S., Osakabe, A., Tachiwana, H., Takizawa, Y., Kagawa, W., Kitao, H., Dohmae, N., et al. (2012a). Histone chaperone activity of Fanconi anemia proteins, FANCD2 and FANCI, is required for DNA crosslink repair. EMBO J. *31*, 3524–3536.

Sato, K., Toda, K., Ishiai, M., Takata, M., and Kurumizaka, H. (2012b). DNA robustly stimulates FANCD2 monoubiquitylation in the complex with FANCI. Nucleic Acids Res. *40*, 4553–4561.

Schaeper, U., Subramanian, T., Lim, L., Boyd, J.M., and Chinnadurai, G. (1998). Interaction between a cellular protein that binds to the C-terminal

Figure 4. Functional Interplay between Monoubiquitinatinaed FANCD2 and CtIP

(A) CoIP between endogenous CtIP and GFP-FANCD2 WT or lacking the monoubiquitination site in Flp-In T-REx 293 cells.

(B) Pull-down assay with purified GST-chicken CtIP (cCtIP) and monoubiquitinated chicken FANCD2 (cFANCD2).

(C) RPA2 phosphorylation in U2OS cells depleted of FANCD2 or CtIP. The ratio of phospho- versus total RPA2 was normalized to the value from the cells treated with control siRNA and MMC. This experiment was repeated twice with similar results.

(D) Clonogenic cell survival. U2OS cells were transfected with the respective siRNAs, as indicated, and after 48 hr stimulated with MMC for an additional 24 hr. Data shown are the mean and SE of three independent experiments.

(E) U2OS cells stably expressing wild-type or mutant siRNA-resistant GFP-CtIP were transfected with siCtIP#2 and tested for MMC sensitivity as in (D). Position of the endogenous CtIP was indicated by the arrowhead. See also Figure S4.

(F) A model of CtIP regulation by the ID complex during ICL repair. See text for details.

region of adenovirus E1A (CtBP) and a novel cellular protein is disrupted by E1A through a conserved PLDLS motif. J. Biol. Chem. *273*, 8549–8552.

Söderberg, O., Gullberg, M., Jarvius, M., Ridderstråle, K., Leuchowius, K.-J., Jarvius, J., Wester, K., Hydbring, P., Bahram, F., Larsson, L.-G., and Landegren, U. (2006). Direct observation of individual endogenous protein complexes in situ by proximity ligation. Nat. Methods *3*, 995–1000.

Stoepker, C., Hain, K., Schuster, B., Hilhorst-Hofstee, Y., Rooimans, M.A., Steltenpool, J., Oostra, A.B., Eirich, K., Korthof, E.T., Nieuwint, A.W.M., et al. (2011). SLX4, a coordinator of structure-specific endonucleases, is mutated in a new Fanconi anemia subtype. Nat. Genet. *43*, 138–141.

Symington, L.S., and Gautier, J. (2011). Double-strand break end resection and repair pathway choice. Annu. Rev. Genet. *45*, 247–271.

Thompson, L.H. (2012). Recognition, signaling, and repair of DNA double-strand breaks produced by ionizing radiation in mammalian cells: the molecular choreography. Mutat. Res. *751*, 158–246.

Vandenberg, C.J., Gergely, F., Ong, C.Y., Pace, P., Mallery, D.L., Hiom, K., and Patel, K.J. (2003). BRCA1-independent ubiquitination of FANCD2. Mol. Cell *12*, 247–254.

Wang, H., Shao, Z., Shi, L.Z., Hwang, P.Y.-H., Truong, L.N., Berns, M.W., Chen, D.J., and Wu, X. (2012). CtIP protein dimerization is critical for its recruitment to chromosomal DNA double-stranded breaks. J. Biol. Chem. *287*, 21471–21480.

Yamamoto, K.N., Kobayashi, S., Tsuda, M., Kurumizaka, H., Takata, M., Kono, K., Jiricny, J., Takeda, S., and Hirota, K. (2011). Involvement of SLX4 in interstrand cross-link repair is regulated by the Fanconi anemia pathway. Proc. Natl. Acad. Sci. USA *108*, 6492–6496.

Yoshikiyo, K., Kratz, K., Hirota, K., Nishihara, K., Takata, M., Kurumizaka, H., Horimoto, S., Takeda, S., and Jiricny, J. (2010). KIAA1018/FAN1 nuclease protects cells against genomic instability induced by interstrand cross-linking agents. Proc. Natl. Acad. Sci. USA *107*, 21553–21557.

You, Z., Shi, L.Z., Zhu, Q., Wu, P., Zhang, Y.-W., Basilio, A., Tonnu, N., Verma, I.M., Berns, M.W., and Hunter, T. (2009). CtIP links DNA double-strand break sensing to resection. Mol. Cell *36*, 954–969.

Yu, X., Fu, S., Lai, M., Baer, R., and Chen, J. (2006). BRCA1 ubiquitinates its phosphorylation-dependent binding partner CtIP. Genes Dev. *20*, 1721–1726.

Zhou, W., Otto, E.A., Cluckey, A., Airik, R., Hurd, T.W., Chaki, M., Diaz, K., Lach, F.P., Bennett, G.R., Gee, H.Y., et al. (2012). FAN1 mutations cause karyomegalic interstitial nephritis, linking chronic kidney failure to defective DNA damage repair. Nat. Genet. *44*, 910–915.

Identification of a novel erythroid-specific enhancer for the *ALAS2* gene and its loss-of-function mutation which is associated with congenital sideroblastic anemia

Kiriko Kaneko,[1,2] Kazumichi Furuyama,[1,6] Tohru Fujiwara,[3] Ryoji Kobayashi,[4] Hiroyuki Ishida,[5] Hideo Harigae,[3] and Shigeki Shibahara[1]

[1]Department of Molecular Biology and Applied Physiology, [2]Department of Endocrinology and Applied Medical Science, [3]Department of Hematology and Rheumatology, Tohoku University Graduate School of Medicine, Sendai, Miyagi; [4]Department of Pediatrics, Sapporo Hokuyu Hospital, Sapporo; [5]Department of Pediatrics, Kyoto Prefectural University of Medicine, Graduate School of Medical Science, Kyoto; and [6]Laboratory of Molecular Biochemistry, Iwate Medical University, Yahaba, Iwate, Japan

ABSTRACT

Erythroid-specific 5-aminolevulinate synthase (ALAS2) is the rate-limiting enzyme for heme biosynthesis in erythroid cells, and a missense mutation of the *ALAS2* gene is associated with congenital sideroblastic anemia. However, the gene responsible for this form of anemia remains unclear in about 40% of patients. Here, we identify a novel erythroid-specific enhancer of 130 base pairs in the first intron of the *ALAS2* gene. The newly identified enhancer contains a *cis*-acting element that is bound by the erythroid-specific transcription factor GATA1, as confirmed by chromatin immunoprecipitation analysis *in vivo* and by electrophoretic mobility shift assay *in vitro*. A promoter activity assay in K562 human erythroleukemia cells revealed that the presence of this 130-base pair region increased the promoter activity of the *ALAS2* gene by 10-15-fold. Importantly, two mutations, each of which disrupts the GATA-binding site in the enhancer, were identified in unrelated male patients with congenital sideroblastic anemia, and the lower expression level of ALAS2 mRNA in bone marrow erythroblasts was confirmed in one of these patients. Moreover, GATA1 failed to bind to each mutant sequence at the GATA-binding site, and each mutation abolished the enhancer function on ALAS2 promoter activity in K562 cells. Thus, a mutation at the GATA-binding site in this enhancer may cause congenital sideroblastic anemia. These results suggest that the newly identified intronic enhancer is essential for the expression of the *ALAS2* gene in erythroid cells. We propose that the 130-base pair enhancer region located in the first intron of the *ALAS2* gene should be examined in patients with congenital sideroblastic anemia in whom the gene responsible is unknown.

Introduction

The *ALAS2* gene encodes for erythroid-specific 5-aminolevulinate synthase (ALAS-E, EC 2.3.1.37), which is the rate-limiting enzyme of the heme biosynthetic pathway in erythroid cells.[1] It has been reported that the human *ALAS2* gene is mapped on the X chromosome,[2] and that a loss-of-function mutation of this gene causes X-linked sideroblastic anemia (XLSA),[3,4] which is the most common genetic form of congenital sideroblastic anemia (CSA). Moreover, a missense mutation of *ALAS2* was identified in a patient with non-familial CSA (nfCSA),[5] in which no family history of sideroblastic anemia was identified. In addition to *ALAS2*, several other genes were recently identified as causative genes for CSA, including *SLC25A38*,[6] *GLRX5*,[7] *ABCB7*,[8] *PUS1*,[9] and *SLC19A2*,[10] but the cause of sideroblastic anemia still remains undefined in more than 40% of patients with CSA.[11]

GATA1 transcription factor regulates the expression of several erythroid-specific genes, such as erythropoietin receptor gene,[12,13] α- and β-globin genes,[14,15] *ALAS2*[16] and the *GATA1* gene itself,[17] during erythroid differentiation.[18,19] Ablation of the *Gata1* gene in mice resulted in embryonic death because of anemia,[20] suggesting that GATA1 is essential for erythroid differentiation *in vivo*. It has been reported that GATA1 regulates transcription of human *ALAS2* through the proximal promoter region[16] and the erythroid-specific enhancer located in the eighth intron of *ALAS2*.[21] However, Fujiwara *et al.* demonstrated that the GATA1 protein binds to the *ALAS2* gene only in the middle of its first intron, where no regulatory region had so far been identified, by genome-wide analysis of K562 human erythroleukemia cells using chromatin immunoprecipitation followed by next-generation sequencing (ChIP-seq).[22]

In the present study, we have identified a novel erythroid-specific enhancer region in the first intron of the *ALAS2* gene. Moreover, we describe two mutations in the newly identified enhancer of *ALAS2*: a T-to-C transition, which changes GATA to GGTA at the GATA element in the antisense strand, in a pedigree with XLSA and one proband with nfCSA, and a 35-base pair (bp) deletion including the above-mentioned GATA element in a proband with nfCSA.

Methods

Polymerase chain reaction

DNA polymerases used for polymerase chain reaction (PCR) analysis were purchased from TAKARA BIO Inc. (Shiga, Japan). The

 doi:10.3324/haematol.2013.085449
The online version of this article has a Supplementary Appendix.
Manuscript received on February 4, 2013. Manuscript accepted on August 1, 2013.
Correspondence: furuyama@iwate-med.ac.jp

sequence of primers and probes used in this study are listed in the *Online Supplementary Tables*.

Polymerase chain reaction-based quantitative chromatin immunoprecipitation

Real-time PCR-based quantitative chromatin immunoprecipitation (ChIP-qPCR) analysis was conducted essentially as previously described.[22]

Electrophoretic mobility shift assay

Electrophoretic mobility shift assay (EMSA) was performed using "DIG Gel Shift Kit, 2nd Generation" (Roche Diagnostics GmbH, Mannheim, Germany), according to the manufacturer's protocol. Sequences of oligonucleotides for probes are indicated by the horizontal bar in the relevant figures. Nuclear extracts were prepared, as described previously,[23] from K562 cells or HEK293 human embryonic kidney cells that were transfected with a GATA1-FLAG fusion protein expression vector or its backbone vector.

Promoter/enhancer activity assays

Each target DNA fragment was prepared from genomic DNA from normal volunteers (WT) or patients with CSA (referred to as "GGTA" or "delGATA" in each reporter construct) and was cloned into pGL3basic plasmid (Promega Corporation, Madison, WI, USA). The human ALAS2 proximal promoter region (g.4820_5115, between -267 and +29 from the transcription start site)[16,24] was cloned into the multiple-cloning site of pGL3basic [referred to as pGL3-AEpro(-267)]. A single DNA fragment (5.2 kbp), carrying the ALAS2 proximal promoter, first exon, first intron and the untranslated region of the second exon, was subcloned into the multiple cloning site of pGL3basic [referred to as pGL3-AEpro(-267)+intron1]. A DNA fragment containing the GATA1-binding region in the first intron of the *ALAS2* gene (corresponding to g.7488_7960), which was defined by ChIP-seq analysis,[22] is referred to as the ChIP-peak. The length of the WT ChIP-peak is 473 bp. In addition, a 130-bp fragment containing ALAS2int1GATA, the consensus sequence for the GATA1-binding site in the ChIP-peak, is referred to as ChIPmini. Several deletion mutants of ChIPmini were prepared using pGL3-AEpro(-267)+ChIPmini(WT) as a template. The pGL3-TKpro plasmid was constructed by cloning herpes simplex virus thymidine kinase promoter into the multiple cloning site of pGL3basic plasmid. Each reporter vector and pEF-RL25 were introduced into K562 cells or HEK293 cells. Luciferase activity was determined using a dual-luciferase reporter system (Promega).

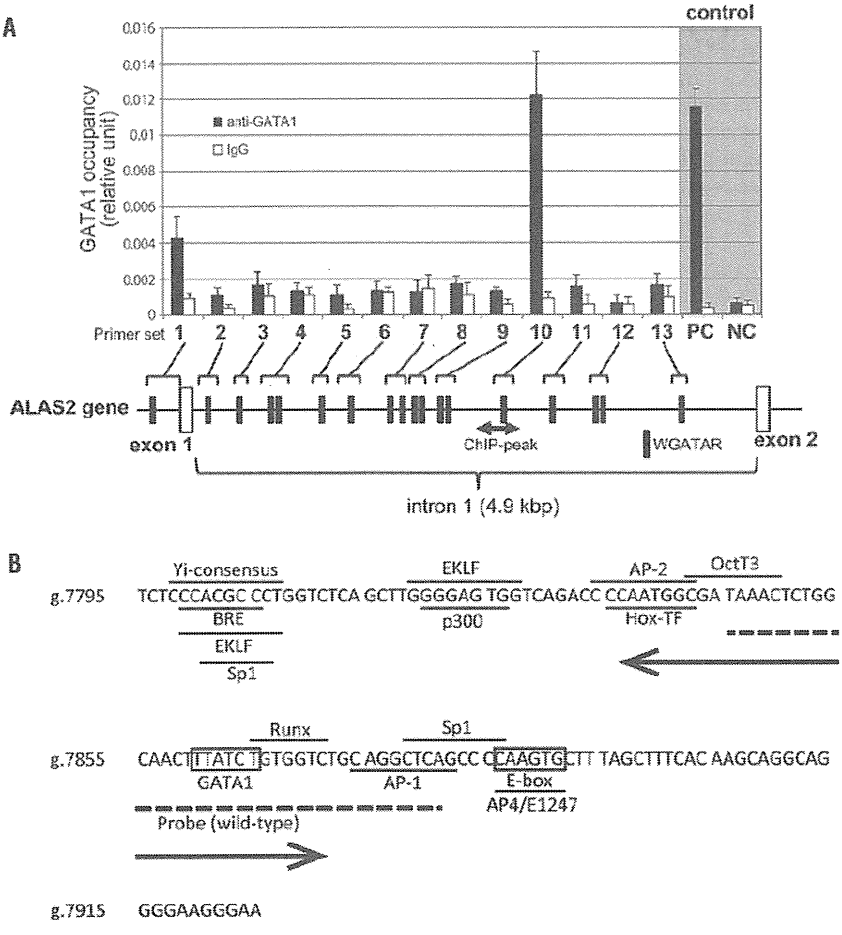

Figure 1. Identification of a functional GATA1 element in the first intron of the *ALAS2* gene. (A) Chromatin immunoprecipitation assay. Fragmented genomic DNA segments were immunoprecipitated with anti-GATA1 antibody or control IgG, and then precipitated fragments were quantified using real-time PCR as described in the *Online Supplementary Methods*. PC or NC indicates positive control or negative control, respectively, for the ChIP assay using anti-GATA1 in K562 cells.[22] One GATA element is present in the proximal promoter region and 17 GATA elements in the first intron (black symbols). The shaded double arrow indicates the region corresponding to ChIP-peak. (B) Nucleotide sequence of ChIPmini. The GATA binding site, ALAS2int1GATA, is located in the center of ChIPmini (boxed). A box also indicates the consensus for E-box that is bound by Scl/TAL1.[22] The sequence of ChIPmini was further analyzed for putative transcription factor binding sites using GeneQuest software (DNASTAR Inc., Madison, WI, USA), and the results are indicated by the horizontal bar. Yi-consensus, Yi transcription factor consensus site;[33] BRE, transcription factor IIB binding site;[34] EKLF, erythroid/Kruppel-like factor consensus site;[35] Sp1, stimulatory protein 1 binding site;[36] P300, P300 transcriptional coactivator consensus site;[37] AP-2, AP-2 beta consensus site;[38] Hox-TF, C1 element binding factor binding site;[39] OctT3, OctT3 binding site;[40] Runx, Runx proteins binding site;[41] AP-1, activator protein 1 binding site;[42] and AP4/E1247, AP4/E1247 binding site.[43] The sequence for the wild-type probe used in the EMSA is indicated by a dashed line. A double arrow indicates the deleted region of the delGATA mutation.

Identification of mutations of the ALAS2 gene

All exons including exon-intron boundaries, the proximal promoter region, and intron 1 and intron 8 of the *ALAS2* gene (GeneBank: NG_8983.1) were directly sequenced according to previously reported methods.[25]

Measurement of ALAS2 mRNA in purified erythroblasts

Total RNA was extracted from glycophorin A-positive bone marrow mononuclear cells, and was used for cDNA synthesis. ALAS2 expression was measured by real-time PCR, and was normalized to that of GAPDH mRNA.

Statistical analysis

Multiple comparisons between groups were made using the Tukey-Kramer test.

Patients

Eleven probands (eight pedigrees) with CSA of unknown cause were selected to determine the nucleotide sequence of the first intron of *ALAS2* gene. In these patients no disease-causative mutation was identified in the coding regions or reported regulatory regions in *ALAS2*, *SLC25A38*, *GLRX5*, *ABCB7*, *PUS1* and *SLC19A2*, which have been reported to be genes causing CSA[11] (see the *Online Supplementary Methods* for full details of the methods).

The genetic analyses performed in this project were approved by the ethical committee of Tohoku University School of Medicine. Blood samples were withdrawn from the probands and the family members after informed consent.

Results

Polymerase chain reaction-based quantitative chromatin immunoprecipitation analysis of the first intron of the ALAS2 gene

To identify the novel regulatory region for ALAS2 tran-

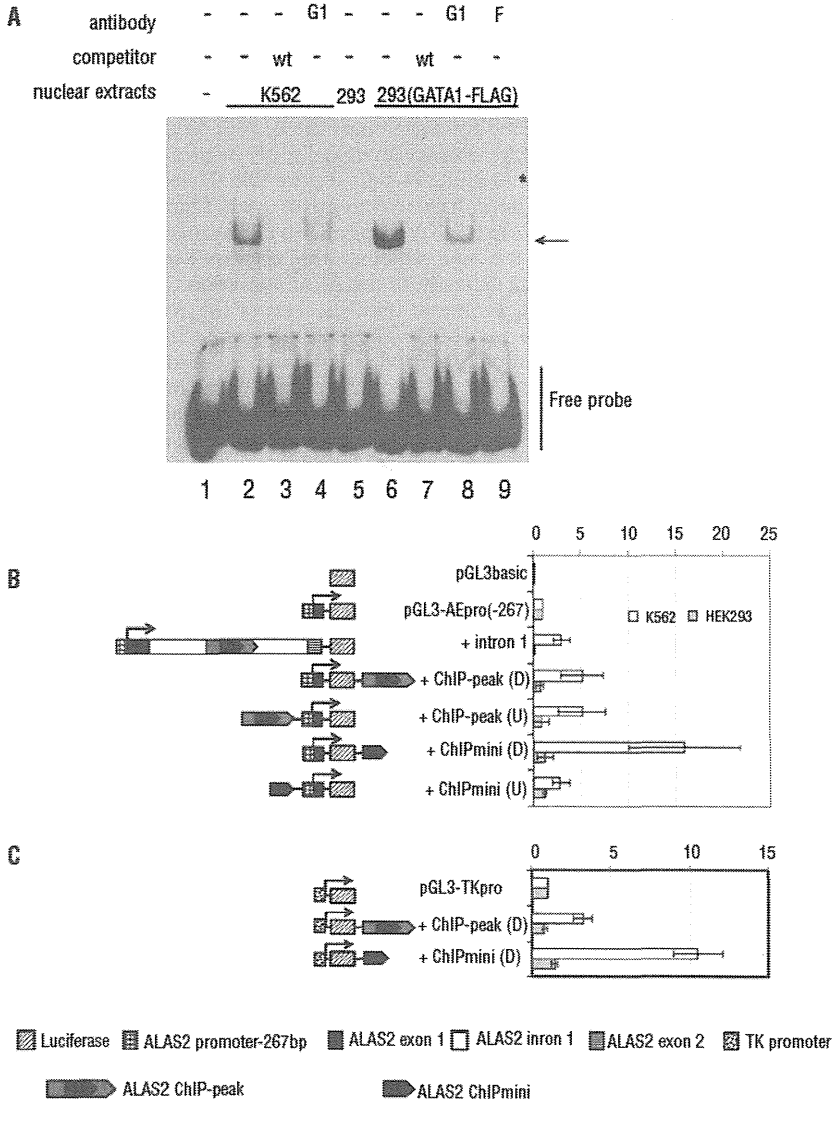

Figure 2. Functional analyses of ChIPmini present in the first intron of the *ALAS2* gene. (A) Electrophoretic mobility shift assay (EMSA). Wild-type (wt) probe was incubated with nuclear extracts prepared from K562 cells (lanes 2-4) or HEK293 cells expressing GATA1-FLAG (lanes 6-9). HEK293 cells were transfected with mock vector (lane 5) or FLAG-fused GATA1 expression vector before preparation of nuclear extracts. The protein-probe complex was detected as a retarded band (arrow). An excess amount of unlabeled probe (lanes 3, 7), anti-GATA1 antibody (G1) (lanes 4, 8) or anti-FLAG antibody (F) (lane 9) was included in the reaction mixture. Lane 1 shows the control without nuclear extracts. The asterisk indicates the super-shifted band (lane 9). (B) Functional analysis of ChIPmini as an enhancer for the *ALAS2* gene. Details of the fragments for each plasmid, such as intron1, ChIP-peak and ChIPmini, are described in the *Methods* section. Each DNA fragment was inserted upstream of the *ALAS2* proximal promoter or downstream of luciferase cDNA, indicated as (U) or (D), respectively. Results are expressed as a relative activity compared to that of pGL3-AEpro(-267), and are presented as the mean ± standard deviation (SD) of three independent experiments. (C) Functional analysis of ChIPmini as an enhancer for non-erythroid gene promoter. The enhancer activity of the first intron was examined using the herpes simplex virus TK promoter as a non-erythroid promoter. ChIP-peak or ChIPmini was inserted downstream of the luciferase gene of pGL3-TKpro, yielding pGL3-TKpro+ChIP-peak(D) or pGL3-TKpro+ChIPmini(D). Each of these reporter vectors was introduced into K562 cells or HEK293 cells to measure enhancer activity. Results are expressed as a relative activity compared to that of pGL3-TKpro, and are presented as the mean ± SD of three independent experiments.

scription, we first performed ChIP-qPCR analysis in K562 cells to localize the GATA1-binding region of the *ALAS2* gene *in vivo*, which was determined by genome-wide ChIP-seq analysis.[22] In fact, ChIP-qPCR enabled us to examine the GATA1-binding activity of an individual GATA element or two adjacent GATA elements in the first intron of the *ALAS2* gene. Based on a search of NCBI Reference Sequence (NG_8983.1) using SeqBuilder software (DNASTAR Inc., Madison, WI, USA), we identified 17 GATA elements (16 out of 17 GATA elements are present in the antisense orientation) in the first intron of human *ALAS2* (Figure 1A), which is compatible with the previous report.[21] We also included the proximal promoter region that contains a functional GATA-binding site (g.4961_4966).[16] Overall 13 primer sets were designed to amplify the GATA elements located in the proximal promoter region and the first intron of *ALAS2* (Figure 1A and *Online Supplementary Table S1*). Among the 12 primer sets targeting the first intron, using primer set 10, we could amplify genomic DNA that was precipitated with anti-GATA1 antibody at a similar level to that of the positive control, but not with other primer sets. We refer to this region amplified with primer set 10 as ChIPmini (g.7795_7924), the sequence of which is shown in Figure 1B. *In silico* analysis identified only one GATA element (g.7860_7865, boxed in Figure 1B) in ChIPmini, termed ALAS2int1GATA. In addition, primer set 1 which targets the proximal promoter region yielded notable amounts of amplified genome DNA. These results indicate that GATA1 protein bound to the regions amplified with primer sets 1 and 10 in K562 cells; that is, GATA1 protein could bind to the proximal promoter region as well as to ALAS2int1GATA in the first intron of the *ALAS2* gene *in vivo*. Since the GATA element located in the proximal promoter has been well examined *in vitro*,[16] we further determined the functional features of ALAS2int1GATA.

GATA1 protein binds to ALAS2int1GATA located in ChIPmini

We then examined whether GATA1 protein binds to ALAS2int1GATA present in the center of ChIPmini using EMSA (Figure 2A). The WT probe contains ALAS2int1GATA (Figure 1B). The incubation of labeled WT probe with nuclear extracts of K562 cells yielded the retarded band that represents the protein-probe complex (lane 2), whereas this retarded band was undetectable with an excess amount of non-labeled WT probe (lane 3). Moreover, the addition of anti-GATA1 antibody reduced the intensity of the retarded band (lane 4), suggesting that GATA1 protein may bind to the WT probe. In fact, the retarded band was not detected when the labeled probe was incubated with nuclear extracts of mock-transfected HEK293 cells (lane 5). In contrast, the retarded band was observed when the labeled probe was incubated with the nuclear extracts of HEK293 cells expressing FLAG-fused GATA1 (lane 6). Importantly, the retarded band observed in lane 6 was not detectable in the presence of an excess amount of non-labeled probe (lane 7). The formation of the retarded band was partially inhibited by anti-GATA1 antibody (lane 8). Likewise, the inclusion of anti-FLAG antibody (lane 9) resulted in the disappearance of the retarded band and instead generated the super-shifted band (indicated by an asterisk). These results suggest that GATA1 protein binds to the WT probe containing ALAS2int1GATA.

Enhancement of ALAS2 promoter activity by the DNA segment containing ALAS2int1GATA

To examine the functional importance of ALAS2int1GATA in the promoter activity of the *ALAS2* gene (Figure 2B), we constructed the pGL3-AEpro(-267) vector, in which the expression of firefly luciferase gene is controlled under the proximal promoter of the *ALAS2* gene (g.4820_5115). The presence of the first intron of *ALAS2* (pGL3-AEpro(-267)+intron1) increased luciferase activity about 3-fold in K562 cells, whereas luciferase activity was decreased to 10% of pGL3-AEpro(-267) in HEK293 cells. When the ChIP-peak, the region determined by ChIP-seq analysis (g.7488_7960),[22] was present downstream [+ChIP-peak(D)] or upstream [+ChIP-peak(U)] of the ALAS2 proximal promoter, luciferase activity was increased about 5-fold, irrespective of the location, compared to that of pGL3-AEpro(-267) in K562 cells. Moreover, the presence of the ChIPmini fragment downstream of the luciferase gene [+ChIPmini (D)] resulted in a 16-fold increase of luciferase activity. However, when the same fragment was inserted upstream of the ALAS2 promoter [+ChIPmini(U)], luciferase activity increased only 3-fold. Thus, the enhancer activity of the ChIPmini fragment varies, depending on its location. Moreover, among the constructs examined, the ChIPmini fragment showed maximum enhancer activity downstream of the luciferase gene. The ChIP-peak or ChIPmini fragment downstream of the ALAS2 promoter influenced luciferase activity marginally (0.73- or 1.25-fold, respectively) in HEK293 cells (Figure 2B). These results suggest that the enhancer activity of each fragment containing ALAS2int1GATA is specific to erythroid cells.

To examine whether the erythroid-specific enhancer activity depends on the ALAS2 promoter, we replaced the ALAS2 promoter with the herpes simplex virus TK promoter (Figure 2C). The ChIP-peak and ChIPmini enhanced TK promoter activity 3.4- and 9.8-fold in K562 cells, respectively, whereas they did not enhance TK promoter activity in HEK293 cells. These results indicate that the erythroid-specific enhancer is present in the ChIP-peak and ChIPmini fragments. In addition, the erythroid-specific enhancer is functional in the non-erythroid gene promoter.

Identification of mutations in the first intron of the ALAS2 gene in patients with congenital sideroblastic anemia

Considering the newly identified enhancer in the first intron of the *ALAS2* gene, we examined whether some CSA patients carry the mutation in ChIP-peak or ChIPmini of *ALAS2*. We determined the nucleotide sequence of the first intron of *ALAS2* in 11 probands (eight pedigrees), and found two distinct mutations in the newly identified enhancer region in five Japanese patients (three pedigrees). The clinical features and hematologic status of the probands at diagnosis of the disease are summarized in Table 1.

Proband 1 in a pedigree with XLSA

The first male Japanese proband was referred to hospital at the age of 3 months to investigate the cause of his pale face. No problems were reported during the birth. Investigations showed microcytic/hypochromic anemia, an increased concentration of serum iron and raised serum ferritin level. Bone marrow aspiration revealed the presence of ring sideroblasts. Two maternal relatives – male cousins of the proband's mother – have sideroblastic ane-

mia (Figure 3A). The pedigree of this family suggested X chromosome-linked inheritance of the disease. The proband's anemia was not improved by pyridoxine administration (5 mg/kg/day for 3 months), and the boy required once monthly transfusions of one unit of concentrated red blood cells to maintain an adequate hemoglobin level. At the age of 7 months, this proband died of sepsis caused by alpha-streptococcus.

Proband 2 with nfCSA

The second male Japanese proband visited hospital at the age of 4 years because of the paleness of his complexion. Investigations showed microcytic/hypochromic anemia, mild thrombocytosis, and a high serum iron concentration with a normal serum ferritin concentration. Bone marrow aspiration revealed the presence of ring sideroblasts (38% of the erythroblasts). Giant platelets were observed in the bone marrow, although dysplasia of the megakaryocytes was not clear. There was no family history of sideroblastic anemia (Figure 3B).

Proband 3 with nfCSA

The third male Japanese proband was noted to have anemia at the age of 2 years, but details are not available. Without any treatment, serum hemoglobin level was maintained at 70 g/L, and increased to 100 g/L at the age of 10. Accordingly, the proband stopped visiting the hospital. At the age of 19, however, the proband was admitted to hospital because of general fatigue. Investigations revealed microcytic, hypochromic anemia with systemic iron overload. The presence of ring sideroblasts was confirmed in his bone marrow by Prussian blue staining (36% of erythroblasts). Although this proband was treated with pyridoxine (150 mg/day) for 8 months, his anemia did not improve. There was no family history of sideroblastic anemia (Figure 3C).

In proband 1 from the pedigree with XLSA (Figure 3A), we identified a single nucleotide mutation (Figure 4, upper panel, g.7863T>C), which alters the core sequence of ALAS2int1GATA in the antisense strand from GATA to GGTA (referred to as "GGTA mutation"). The same mutation of the *ALAS2* gene was also identified in two cousins of the proband's mother, both of whom were diagnosed as having sideroblastic anemia (Figure 3A). Clinical specimens for genetic analysis were not available from either the parents or the elder brother of proband 1.

The same GGTA mutation was identified at ALAS2int1GATA in proband 2 with CSA (Figure 4, middle panel). There was no known consanguinity between proband 1 and proband 2. Genomic DNA from the parents of proband 2 was not available, because they did not agree to provide their clinical specimens for genetic analysis. Since proband 2 was also noted to have thrombocytosis (Table 1), we searched for a *JAK2* mutation in the genomic DNA extracted from the peripheral blood of this patient. However, no V617F mutation or any missense

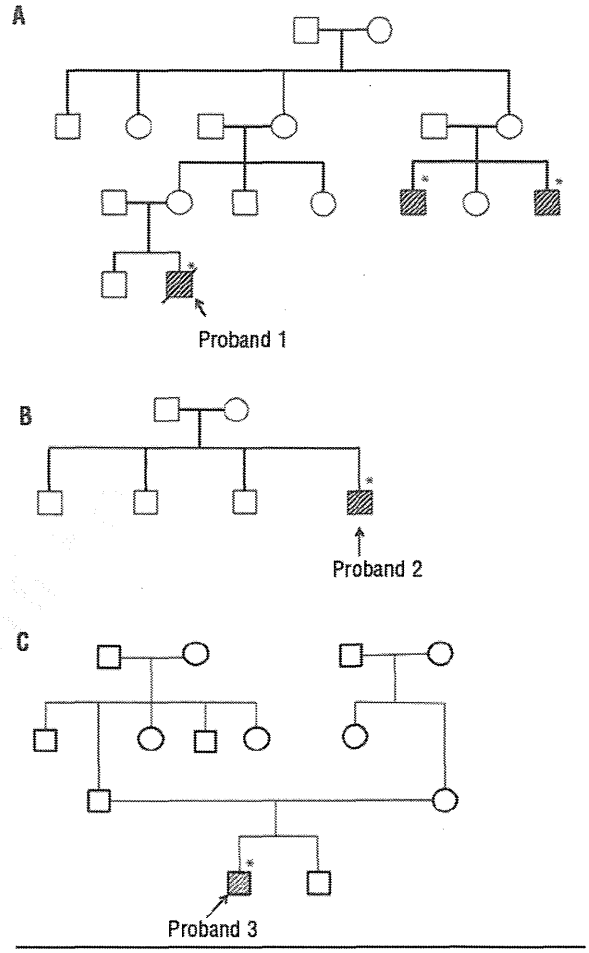

Figure 3. Family trees of three unrelated probands. Family tree of: (A) proband 1 with XLSA, (B) proband 2 with nfCSA, and (C) proband 3 with nfCSA. Shaded boxes indicate affected individuals in each pedigree. Asterisks indicate the individuals in whom a mutation in the first intron of the *ALAS2* gene was detected.

Table 1. Hematologic status of each proband at diagnosis of the disease.

	Onset of the anemia	Age at diagnosis of SA	Family history of XLSA	Hb (g/L)	MCV (fL)	MCH (pg)	Platelets ($x10^9$/L)	Serum iron (μmol/L)	Ferritin (pmol/L)
Proband 1	4 months	4 months	yes	39 [136-183]	65 [83-101]	18.7 [28-35]	246 [140-379]	63.9 [10.7-37.6]	399.7 [49.4-270]
Proband 2	4 years	4 years	no	84 [126-165]	73.4 [87-104]	22 [29-35]	610 [138-309]	49.1 [12.5-25.0]	670.1 [67.4-725]
Proband 3	2 years	19 years	no	78 [120-165]	73.9 [80-100]	22.2 [28-34]	373 [160-420]	39.6 [14.3-21.5]	2489.7 [40.4-288]

The normal value of each clinical examination is shown in brackets. SA: sideroblastic anemia; XLSA: X-linked sideroblastic anemia; Hb: hemoglobin; MCV: mean corpuscular volume; MCH: mean corpuscular hemoglobin.

mutation in exon 12, each of which is frequently observed in patients with refractory anemia with ring sideroblasts and thrombocytosis (RARS-T),[27] was detected (*data not shown*). Thus, the GGTA mutation at ALAS2int1GATA may be responsible for the sideroblastic anemia in proband 2.

In proband 3 with CSA, a deletion of 35 bp was identified in the first intron of the *ALAS2* gene (Figure 4A, lower panel, g.7836_7870del, referred to as "delGATA mutation"). The delGATA mutation results in the loss of ALAS2int1GATA. However, the delGATA mutation was not identified in the *ALAS2* gene of the parents of proband 3 (*data not shown*). Thus, the delGATA mutation may be a *de novo* mutation or a somatic mutation. Accordingly, we compared the relative ALAS2 mRNA level in the erythroid progenitor cells isolated from proband's bone marrow with those of normal subjects. The ALAS2 mRNA level was more than 7-fold lower in the proband's erythroblasts than in those of three independent, normal subjects (Figure 4B), suggesting that the delGATA mutation may lead to decreased transcription of the *ALAS2* gene.

Lastly, we examined the sequence of the region corresponding to g.7513_8165 of the *ALAS2* gene, which contains ChIPmini, in 103 healthy, Japanese volunteers (44 males and 59 females, total 162 alleles) using PCR followed by direct sequencing. No mutation was found in this region (*data not shown*). In addition, no single nucleotide polymorphism was reported in this GATA element, based on the single nucleotide polymorphism database available at the NCBI home page (*http://www.ncbi.nlm.nih.gov/snp*, current assembly is GRCh37.p5). Thus, the GGTA mutation and delGATA mutation at ALAS2int1GATA may be unique to patients with sideroblastic anemia. Taken together, we suggest that the newly identified mutations at ALAS2int1GATA are responsible for sideroblastic anemia.

The mutation at ALAS2int1GATA impairs GATA1-binding activity and enhancer function

We examined the effect of the GGTA mutation or the delGATA mutation on the binding of GATA1 protein to ALAS2int1GATA using each mutant probe (Figure 5A). The delGATA probe represents the 5'- and 3'-flanking sequences of the deleted 35-bp segment (see Figure 4A). As shown in Figure 5B, the incubation of labeled WT probe with nuclear extracts from HEK293 cells expressing FLAG-fused GATA1

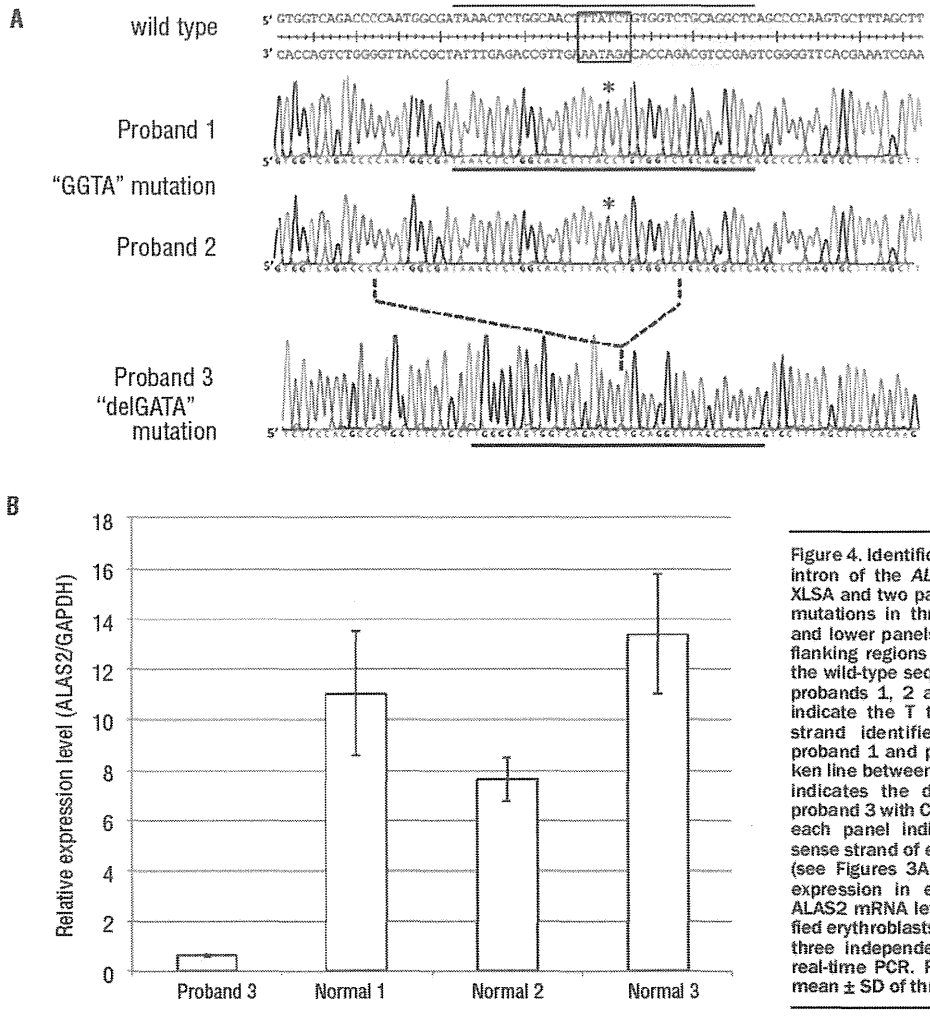

Figure 4. Identification of mutations in the first intron of the *ALAS2* gene in a patient with XLSA and two patients with nfCSA. (A) *ALAS2* mutations in three probands. Upper, middle and lower panels show the sequences of the flanking regions of ALAS2int1GATA (boxed in the wild-type sequence) in the *ALAS2* gene of probands 1, 2 and 3, respectively. Asterisks indicate the T to C transition in the sense strand identified in the *ALAS2* gene of proband 1 and proband 2 with CSA. The broken line between the middle and lower panels indicates the deleted region identified in proband 3 with CSA. The solid horizontal bar in each panel indicates the sequence of the sense strand of each probe used for the EMSA (see Figures 3A and 5B). (B) ALAS2 mRNA expression in erythroblasts of proband 3. ALAS2 mRNA levels were determined in purified erythroblasts isolated from proband 3 and three independent normal individuals using real-time PCR. Results are expressed as the mean ± SD of three independent experiments.

showed a retarded band (lane 3): this band was super-shifted by the addition of anti-FLAG antibody (lane 4), or undetectable with non-labeled WT probe (lane 5), whereas the non-labeled GGTA probe (lane 6) or delGATA probe (lane 7) could not compete for the labeled WT probe. Furthermore, the retarded band was not detectable when labeled GGTA probe (lane 8) or delGATA probe (lane 9) was incubated with the nuclear extracts of HEK293 cells expressing FLAG-fused GATA1. These results suggest that either the GGTA mutation or the delGATA mutation may impair the binding of GATA1 to ALAS2int1GATA.

We then examined the influence of the point mutation or deletion of ALAS2int1GATA on the enhancing activity of the first intron of the *ALAS2* gene (Figure 6A). The GGTA mutation decreased the enhancing activity of the first intron, ChIP-peak or ChIPmini in K562 cells to 17.0%, 18.5% or 12.9%, respectively, of that of the WT construct. The delGATA mutation decreased the enhancing activity of the first intron of *ALAS2*, ChIP-peak or ChIPmini in K562 cells to 10.5%, 15.7% or 12.6%, respectively, of that of the WT construct. In contrast, the relative luciferase activity of the construct carrying each mutation was only marginally different from that of WT intron 1, ChIP-peak or ChIPmini in HEK293 cells (Figure 6A), thereby confirming that ALAS2int1GATA functions as an erythroid-specific enhancer.

There are several potential *cis*-elements at the flanking regions of ALAS2int1GATA, such as EKLF and Sp1, each of which may be involved in the erythroid-specific transcriptional regulation of the *ALAS2* gene.[16,21] We thus analyzed the roles of these *cis*-elements in the enhancer activity of ALAS2int1GATA using deletion mutants at the 5'- or 3'-flanking region of ChIPmini, constructed in pGL3-AEpro(-267)+ChIPmini(D). Deletion of the EKLF1 element at the 5'-flanking region or both E-box and Sp1 elements at the 3'-flanking region did not significantly influence the enhancer activity of ChIPmini (Figure 6B). It should be noted that the Sp1 site overlaps with the 3'-portion of the AP-1 site and the 5'-portion of the E-box (Figure 6C). Moreover, deletion at the 5'-flanking region of ChIPmini ("delEKLF2", "delAP2" and "delOctT3") marginally decreased the enhancer activity (Figure 6B), but the change was not statistically significant. In contrast, deletion of the AP-1 element at the 3'-flanking region ("delAP1" in Figure 6B) significantly decreased the enhancer activity, by about 40% of the activity of ChIPmini(WT). The significant decrease of enhancer activity was observed only in ChIPmini(GGTA), ChIPmini(delGATA) and delAP1, compared to the activity of ChIPmini(WT) (*P<0.05 and **P<0.01 in Figure 6B). We next constructed another reporter vector that carries an internal deletion of the 5' portion of the AP-1 element with an intact Sp1 site ("lackAP1" in Figure 6B). Internal deletion of the AP-1 element alone in ChIPmini decreased the enhancer activity, although not to a statistically significant degree. Thus, the entire AP-1 element seems to be important for the

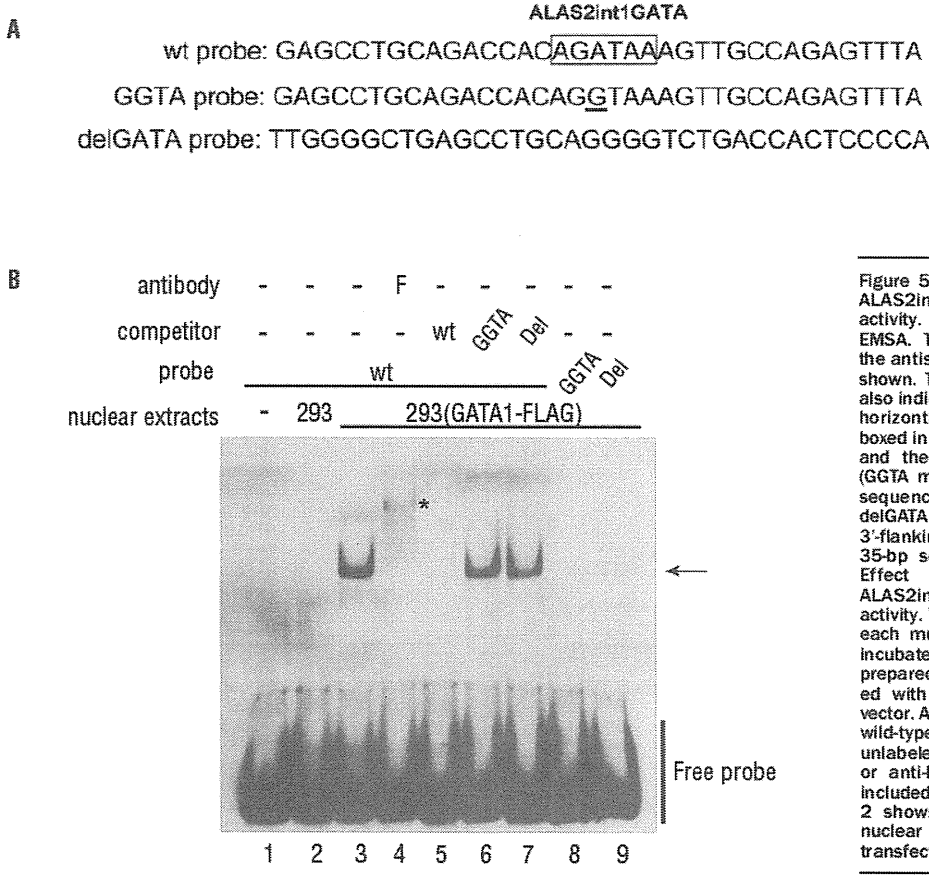

Figure 5. Effects of the mutations of ALAS2int1GATA on GATA1-binding activity. (A) DNA probes used in the EMSA. The nucleotide sequences in the antisense strand of the probes are shown. The position of each probe is also indicated in Figure 1B as the solid horizontal bar. ALAS2int1GATA is boxed in the sequence of the wt probe, and the single nucleotide transition (GGTA mutation) is underlined in the sequence of the GGTA probe. The delGATA probe represents the 5'- and 3'-flanking sequences of the deleted 35-bp segment (see Figure 3B). (B) Effect of each mutation of ALAS2int1GATA on GATA1-binding activity. Wild-type probe (lanes 3-7) or each mutant probe (lanes 8, 9) was incubated with the nuclear extracts prepared from HEK293 cells transfected with the GATA1-FLAG expression vector. An excess amount of unlabeled wild-type probe (lane 5), each of the unlabeled mutant probes (lanes 6, 7), or anti-FLAG antibody (lane 4) was included in the reaction mixture. Lane 2 shows the negative control with nuclear extracts from HEK293 cells transfected with mock vector.

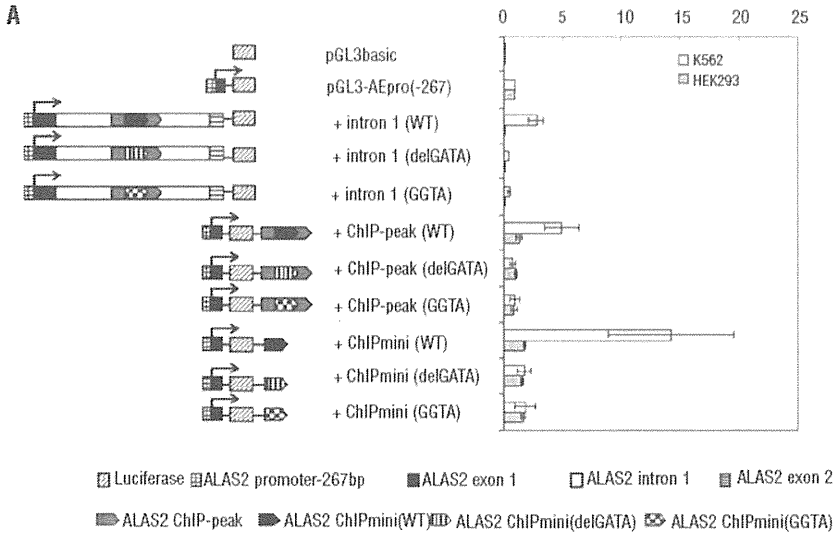

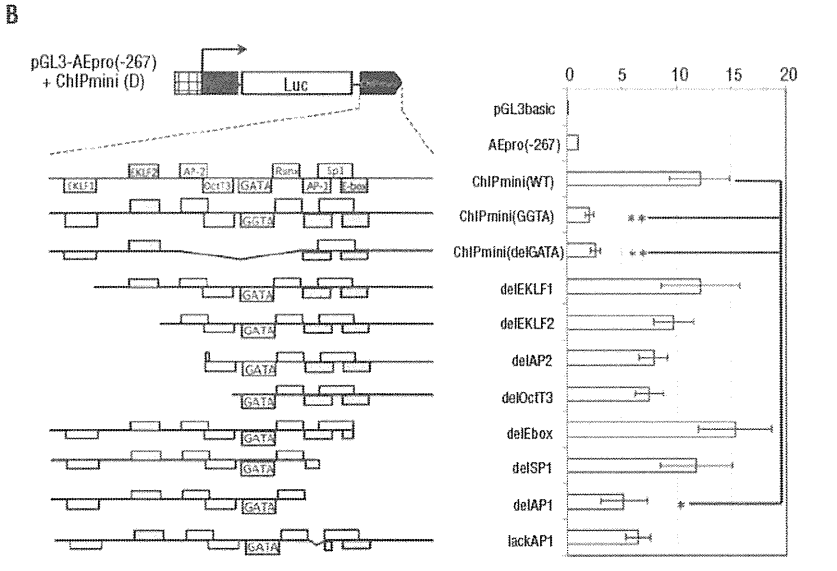

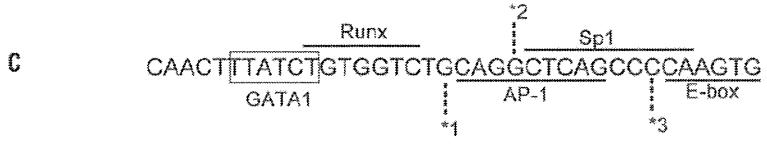

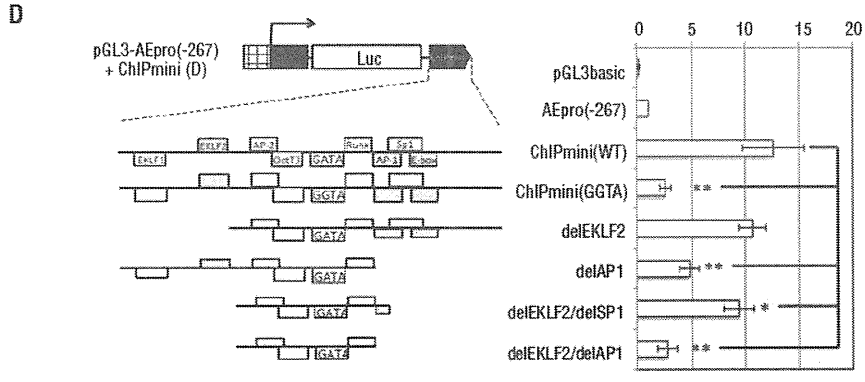

Figure 6. Identification of *cis*-elements essential for the erythroid-specific enhancer activity of ChIPmini. (A) Effect of each mutation of ALAS2int1GATA on the enhancer activity of *ALAS2* ChIPmini. The region corresponding to +intron1, ChIP-peak or ChIPmini, derived from proband 1 or proband 3, was subcloned into pGL3-AEpro(-267) to construct the reporter vector containing the GGTA mutation or the deletion of ALAS2int1GATA, respectively. (B) Effect of the deletion at the 5'- or 3'-flanking region of ALAS2int1GATA on the enhancer activity of ChIPmini. The 5'- and 3'-flanking regions of ALAS2int1GATA contain potential transcription factor-binding sites (*cis*-elements), and a portion of each flanking region was deleted, as schematically shown. The enhancer activity of each deletion mutant was determined in K562 erythroleukemia cells. (C) The nucleotide sequence of the 3'-flanking region of ALAS2int1GATA. Note that the Sp1 site overlaps the AP-1 site and E-box. Each number, *1, *2 or *3, indicates the nucleotide at the 3' end of the deletion mutant, delAP1, delSP1 or delE-box, respectively. Thus, delSP1 also lacks the 3' portion of the AP-1 site. (D) Effect of deletion of the 5'- and 3'-flanking regions of ALAS2int1GATA on the enhancer activity of ChIPmini. The construct, delEKLF2/delSP1, lacks two EKLF sites in the 5'-flanking region and both the Sp1 element and E-box in the 3'-flanking region. The AP-1 element at the 3'-flanking region was deleted from delEKLF2/delSP1, yielding delEKLF2/delAP1. Results are expressed as relative activity compared to that of pGL3-AEpro(-267), and are presented as the mean ± SD of at least three independent experiments.

enhancer activity of ChIPmini (WT) (Figure 6B).

Consequently, we constructed delEKLF2/delSP1 and delELKLF2/delAP1, each of which lacks EKLF elements at the 5'-flanking region and the Sp1 element or the AP-1 element at the 3'-flanking region, respectively (Figure 6D). The deletion mutant, delEKLF2/delSP1, still retained enhancer activity at about 80% of that of ChIPmini(WT), whereas delEKLF2/delAP1 showed decreased enhancer activity similar to the activity of ChIPmini(GGTA). These data indicate that ALAS2int1GATA and its flanking region, especially the AP-1 element, are critically important for the erythroid-specific enhancer activity of ChIPmini.

Taken together, these results suggest that the ChIPmini region acts as an erythroid-specific enhancer for the *ALAS2* promoter, and that both the GGTA mutation and the delGATA mutation represent loss-of-function mutations of ALAS2int1GATA.

Discussion

In the present study, we identified an erythroid-specific enhancer region in the first intron of the human *ALAS2* gene (a 130 bp region referred to as ChIPmini), a region which contains ALAS2int1GATA, a functional GATA1-binding site. We also identified the GGTA mutation and the delGATA mutation at ALAS2int1GATA, each of which is associated with XLSA or CSA. Moreover, we confirmed that each mutation diminished the binding of GATA1 transcription factor to ALAS2int1 (Figure 5B) and decreased enhancer activity of ChIPmini (Figure 6A). Thus, the GGTA mutation and delGATA mutation are loss-of function mutations of the *ALAS2* gene. In fact, the expression of ALAS2 mRNA in bone marrow erythroblasts was lower in proband 3 (Figure 4B) than in normal controls. Thus, each loss-of function mutation may lead to decreased transcription of the *ALAS2* gene, thereby causing sideroblastic anemia in male patients. Such a molecular basis is consistent in part with the lack of pyridoxine responsiveness in these patients (see "Patients" section).

The intronic enhancer, ChIPmini, increased ALAS2 promoter activity most efficiently in erythroid cells when it was present downstream of the promoter (Figure 2B). ChIPmini contains potential *cis*-acting elements, including two EKLF-binding sites, each of which overlaps with the Sp1-binding site or p300-binding site, AP-2 site, OctT3 site Runx site, AP-1 binding site, Sp1 site, and E-box (Figure 1B). Further analysis using deletion mutants of ChIPmini revealed that the potential AP-1 binding site at the 3'-flanking region might be involved in the erythroid-specific enhancer activity of ChIPmini (Figure 6B). These results suggest that ALAS2int1GATA and its 3'-flanking region are essential for the erythroid-specific enhancer activity of ChIPmini. In fact, EKLF[28] and AP-1[29] are involved in erythroid-specific gene expression. It is interesting that the inclusion of the whole first intron of the *ALAS2* gene in a reporter construct resulted in a decrease of ALAS2 promoter activity [11% of pGL3-AEpro(-267)] in non-erythroid HEK293 cells (Figures 2B and 6A). Likewise, the ChIP-peak upstream or downstream of the promoter also reduced the promoter activity in HEK293 cells [73% or 88% of pGL3-AEpro(-267), respectively] (Figure 2B). These results suggest that the first intron of the *ALAS2* gene may contain suppressor element(s) in addition to the erythroid-specific enhancer, although the mechanism of the suppression and the relevant region remain elusive.

We have successfully identified a novel erythroid-specific enhancer for ALAS2 expression, and have identified disease-causative mutations of this enhancer in patients with CSA. Despite the fact that about 50 missense or non-sense mutations of the *ALAS2* gene have been reported as disease-causative mutations in patients with XLSA,[3,30] a mutation in the regulatory region for the transcription of *ALAS2* has rarely been reported to date. Ducamp *et al.* reported a 48-bp deletion of the *ALAS2* gene at the proximal promoter region (c.-91_-44del) in a patient with XLSA, and proposed that the identified deletion would cause XLSA, since the level of ALAS2 mRNA in the proband's bone marrow was lower than that of normal controls.[31] In this context, it has been reported that the deleted region contained a functionally important element for ALAS2 transcription.[16] Bekri *et al.* reported a C-to-G transversion at nucleotide -206 (c.-258C>G) from the transcription start site in the proximal region of the human *ALAS2* gene in patients with XLSA;[24] however, May *et al.* identified this transversion in normal individuals from South Wales at the rate of 0.05, suggesting that this promoter mutation is a polymorphism.[32]

In conclusion, we have identified a novel erythroid-specific enhancer in the first intron of the human *ALAS2* gene, the enhancer function of which may be directed by GATA1 with other transcription factors, such as EKLF and AP-1 binding proteins. Furthermore, we identified the loss-of-function mutation of ALAS2int1GATA, the GATA element within this enhancer, in five of 11 patients with CSA in whom the gene responsible could not be identified. Thus, the intronic region containing ALAS2int1GATA of the *ALAS2* gene should be examined in patients with XLSA or nfCSA in whom the genetic mutation causing the sideroblastic anemia is unknown.

Acknowledgments

This work was supported in part by a Grant-in-Aid for Scientific Research (C) (to KF) and Health and Labour Sciences Research Grants (to HH and KF). The authors thank Prof. Norio Komatsu (Juntendo University) for examination for the JAK2 mutation. We are also grateful to the Biomedical Research Core of Tohoku University Graduate School of Medicine for allowing us to use various facilities.

Authorship and Disclosures

Information on authorship, contributions, and financial & other disclosures was provided by the authors and is available with the online version of this article at www.haematologica.org.

References

1. Anderson KE, Sassa S, Bishop DF, Desnick RJ. Disorders of heme biosynthesis: X-linked sideroblastic anemia and the porphyrias. In: Scriver CR, Beaudet AL, Sly WS, Valle D, eds. The Metabolic & Molecular Bases of Inherited Disease. New York: McGraw-Hill Medical Publishing Division, 2001:2991-3062.
2. Cotter PD, Willard HF, Gorski JL, Bishop DF. Assignment of human erythroid delta-aminolevulinate synthase (ALAS2) to a distal subregion of band Xp11.21 by PCR analysis of somatic cell hybrids containing X; autosome translocations. Genomics. 1992;13(1):211-2.

3. Bottomley SS. Sideroblastic Anemias. In: Greer JP, Foerster J, Rogers GM, Paraskevas F, Glader B, Arber DA, et al., eds. Wintrobe's clinical hematology. 12th ed. Philadelphia l London: Wolters Kluwer Health/Lippincott Williams & Wilkins, 2009:835-56.
4. Ohba R, Furuyama K, Yoshida K, Fujiwara T, Fukuhara N, Onishi Y, et al. Clinical and genetic characteristics of congenital sideroblastic anemia: comparison with myelodysplastic syndrome with ring sideroblast (MDS-RS). Ann Hematol. 2013;92(1):1-9.
5. Harigae H, Furuyama K, Kudo K, Hayashi N, Yamamoto M, Sassa S, et al. A novel mutation of the erythroid-specific gamma-aminolevulinate synthase gene in a patient with non-inherited pyridoxine-responsive sideroblastic anemia. Am J Hematol. 1999;62(2):112-4.
6. Guernsey DL, Jiang H, Campagna DR, Evans SC, Ferguson M, Kellogg MD, et al. Mutations in mitochondrial carrier family gene SLC25A38 cause nonsyndromic autosomal recessive congenital sideroblastic anemia. Nat Genet. 2009;41(6):651-3.
7. Camaschella C, Campanella A, De Falco L, Boschetto L, Merlini R, Silvestri L, et al. The human counterpart of zebrafish shiraz shows sideroblastic-like microcytic anemia and iron overload. Blood. 2007;110(4):1353-8.
8. Allikmets R, Raskind WH, Hutchinson A, Schueck ND, Dean M, Koeller DM. Mutation of a putative mitochondrial iron transporter gene (ABC7) in X-linked sideroblastic anemia and ataxia (XLSA/A). Hum Mol Genet. 1999;8(5):743-9.
9. Bykhovskaya Y, Casas K, Mengesha E, Inbal A, Fischel-Ghodsian N. Missense mutation in pseudouridine synthase 1 (PUS1) causes mitochondrial myopathy and sideroblastic anemia (MLASA). Am J Hum Genet. 2004;74(6):1303-8.
10. Labay V, Raz T, Baron D, Mandel H, Williams H, Barrett T, et al. Mutations in SLC19A2 cause thiamine-responsive megaloblastic anaemia associated with diabetes mellitus and deafness. Nat Genet. 1999;22(3):300-4.
11. Bergmann AK, Campagna DR, McLoughlin EM, Agarwal S, Fleming MD, Bottomley SS, et al. Systematic molecular genetic analysis of congenital sideroblastic anemia: evidence for genetic heterogeneity and identification of novel mutations. Pediatr Blood Cancer. 2010;54(2):273-8.
12. Zon LI, Youssoufian H, Mather C, Lodish HF, Orkin SH. Activation of the erythropoietin receptor promoter by transcription factor GATA-1. Proc Natl Acad Sci USA. 1991;88(23):10638-41.
13. Chiba T, Ikawa Y, Todokoro K. GATA-1 transactivates erythropoietin receptor gene, and erythropoietin receptor-mediated signals enhance GATA-1 gene expression. Nucleic Acids Res. 1991;19(14):3843-8.
14. Evans T, Felsenfeld G. The erythroid-specific transcription factor eryf1: a new finger protein. Cell. 1989;58(5):877-85.
15. Whitelaw E, Tsai SF, Hogben P, Orkin SH. Regulated expression of globin chains and the erythroid transcription factor GATA-1 during erythropoiesis in the developing mouse. Mol Cell Biol. 1990;10(12):6596-606.
16. Surinya KH, Cox TC, May BK. Transcriptional regulation of the human erythroid 5-aminolevulinate synthase gene. Identification of promoter elements and role of regulatory proteins. J Biol Chem. 1997;272(42):26585-94.
17. Kobayashi M, Nishikawa K, Yamamoto M. Hematopoietic regulatory domain of gata1 gene is positively regulated by GATA1 protein in zebrafish embryos. Development. 2001;128(12):2341-50.
18. Ohneda K, Yamamoto M. Roles of hematopoietic transcription factors GATA-1 and GATA-2 in the development of red blood cell lineage. Acta Haematol. 2002;108(4):237-45.
19. Weiss MJ, Keller G, Orkin SH. Novel insights into erythroid development revealed through in vitro differentiation of GATA-1 embryonic stem cells. Genes Dev. 1994;8(10):1184-97.
20. Fujiwara Y, Browne CP, Cunniff K, Goff SC, Orkin SH. Arrested development of embryonic red cell precursors in mouse embryos lacking transcription factor GATA-1. Proc Natl Acad Sci USA. 1996;93(22):12355-8.
21. Surinya KH, Cox TC, May BK. Identification and characterization of a conserved erythroid-specific enhancer located in intron 8 of the human 5-aminolevulinate synthase 2 gene. J Biol Chem. 1998;273(27):16798-809.
22. Fujiwara T, O'Geen H, Keles S, Blahnik K, Linnemann AK, Kang YA, et al. Discovering hematopoietic mechanisms through genome-wide analysis of GATA factor chromatin occupancy. Mol Cell. 2009;36(4):667-81.
23. Vargas PD, Furuyama K, Sassa S, Shibahara S. Hypoxia decreases the expression of the two enzymes responsible for producing linear and cyclic tetrapyrroles in the heme biosynthetic pathway. FEBS J. 2008;275(23):5947-59.
24. Bekri S, May A, Cotter PD, Al-Sabah AI, Guo X, Masters GS, et al. A promoter mutation in the erythroid-specific 5-aminolevulinate synthase (ALAS2) gene causes X-linked sideroblastic anemia. Blood. 2003;102(2):698-704.
25. Muto A, Hoshino H, Madisen L, Yanai N, Obinata M, Karasuyama H, et al. Identification of Bach2 as a B-cell-specific partner for small maf proteins that negatively regulate the immunoglobulin heavy chain gene 3' enhancer. EMBO J. 1998;17(19):5734-43.
26. Kadirvel S, Furuyama K, Harigae H, Kaneko K, Tamai Y, Ishida Y, et al. The carboxyl-terminal region of erythroid-specific 5-aminolevulinate synthase acts as an intrinsic modifier for its catalytic activity and protein stability. Exp Hematol. 2012;40(6):477-86 e1.
27. Szpurka H, Tiu R, Murugesan G, Aboudola S, Hsi ED, Theil KS, et al. Refractory anemia with ringed sideroblasts associated with marked thrombocytosis (RARS-T), another myeloproliferative condition characterized by JAK2 V617F mutation. Blood. 2006;108(7):2173-81.
28. Miller IJ, Bieker JJ. A novel, erythroid cell-specific murine transcription factor that binds to the CACCC element and is related to the Kruppel family of nuclear proteins. Mol Cell Biol. 1993;13(5):2776-86.
29. Ney PA, Sorrentino BP, McDonagh KT, Nienhuis AW. Tandem AP-1-binding sites within the human beta-globin dominant control region function as an inducible enhancer in erythroid cells. Genes Dev. 1990;4(6):993-1006.
30. Harigae H, Furuyama K. Hereditary sideroblastic anemia: pathophysiology and gene mutations. Int J Hematol. 2010;92(3):425-31.
31. Ducamp S, Kannengiesser C, Touati M, Garcon L, Guerci-Bresler A, Guichard JF, et al. Sideroblastic anemia: molecular analysis of the ALAS2 gene in a series of 29 probands and functional studies of 10 missense mutations. Hum Mutat. 2011;32(6):590-7.
32. May A, Barton C, Masters G, Kingston J, Lawless S, Jenner M. Severe sideroblastic anaemia in an ALAS2 compound heterozygote for -206G, a common polymorphism, and a novel mutation in exon 11 (Lys535del) linked to lack of haemoglobinisation in vitro and ineffective erythropoiesis in vivo. Blood (ASH Annual Meeting Abstracts). 2005;106(11):3541.
33. Dou QP, Fridovich-Keil JL, Pardee AB. Inducible proteins binding to the murine thymidine kinase promoter in late G1/S phase. Proc Natl Acad Sci USA. 1991;88(4):1157-61.
34. Lagrange T, Kapanidis AN, Tang H, Reinberg D, Ebright RH. New core promoter element in RNA polymerase II-dependent transcription: sequence-specific DNA binding by transcription factor IIB. Genes Dev. 1998;12(1):34-44.
35. Gallagher PG, Sabatino DE, Romana M, Cline AP, Garrett LJ, Bodine DM, et al. A human beta-spectrin gene promoter directs high level expression in erythroid but not muscle or neural cells. J Biol Chem. 1999;274(10):6062-73.
36. Faisst S, Meyer S. Compilation of vertebrate-encoded transcription factors. Nucleic Acids Res. 1992;20(1):3-26.
37. Rikitake Y, Moran E. DNA-binding properties of the E1A-associated 300-kilodalton protein. Mol Cell Biol. 1992;12(6):2826-36.
38. Moser M, Imhof A, Pscherer A, Bauer R, Amselgruber W, Sinowatz F, et al. Cloning and characterization of a second AP-2 transcription factor: AP-2 beta. Development. 1995;121(9):2779-88.
39. Gilthorpe J, Vandromme M, Brend T, Gutman A, Summerbell D, Totty N, et al. Spatially specific expression of Hoxb4 is dependent on the ubiquitous transcription factor NFY. Development. 2002;129(16):3887-99.
40. Nallur GN, Prakash K, Weissman SM. Multiplex selection technique (MuST): an approach to clone transcription factor binding sites. Proc Natl Acad Sci USA. 1996;93(3):1184-9.
41. Sorensen KD, Quintanilla-Martinez L, Kunder S, Schmidt J, Pedersen FS. Mutation of all Runx (AML1/core) sites in the enhancer of T-lymphomagenic SL3-3 murine leukemia virus unmasks a significant potential for myeloid leukemia induction and favors enhancer evolution toward induction of other disease patterns. J Virol. 2004;78(23):13216-31.
42. Spandidos DA, Yiagnisis M, Pintzas A. Human immunodeficiency virus long terminal repeat responds to transformation by the mutant T24 H-ras1 oncogene and it contains multiple AP-1 binding TPA-inducible consensus sequence elements. Anticancer Res. 1989;9(2):383-6.
43. Mullhaupt B, Feren A, Jones A, Fodor E. DNA sequence and functional characterization of the human and rat epidermal growth factor promoter: regulation by cell growth. Gene. 2000;250(1-2):191-200.

Genetic correction of *HAX1* in induced pluripotent stem cells from a patient with severe congenital neutropenia improves defective granulopoiesis

Tatsuya Morishima,[1] Ken-ichiro Watanabe,[1] Akira Niwa,[2] Hideyo Hirai,[3] Satoshi Saida,[1] Takayuki Tanaka,[2] Itaru Kato,[1] Katsutsugu Umeda,[1] Hidefumi Hiramatsu,[1] Megumu K. Saito,[2] Kousaku Matsubara,[4] Souichi Adachi,[5] Masao Kobayashi,[6] Tatsutoshi Nakahata,[2] and Toshio Heike[1]

[1]Department of Pediatrics, Graduate School of Medicine, Kyoto University, Kyoto; [2]Department of Clinical Application, Center for iPS Cell Research and Application, Kyoto University, Kyoto; [3]Department of Transfusion Medicine and Cell Therapy, Kyoto University Hospital, Kyoto; [4]Department of Pediatrics, Nishi-Kobe Medical Center, Kobe; [5]Human Health Sciences, Graduate School of Medicine, Kyoto University, Kyoto; and [6]Department of Pediatrics, Hiroshima University Graduate School of Biomedical Sciences, Hiroshima, Japan

ABSTRACT

HAX1 was identified as the gene responsible for the autosomal recessive type of severe congenital neutropenia. However, the connection between mutations in the *HAX1* gene and defective granulopoiesis in this disease has remained unclear, mainly due to the lack of a useful experimental model for this disease. In this study, we generated induced pluripotent stem cell lines from a patient presenting for severe congenital neutropenia with *HAX1* gene deficiency, and analyzed their *in vitro* neutrophil differentiation potential by using a novel serum- and feeder-free directed differentiation culture system. Cytostaining and flow cytometric analyses of myeloid cells differentiated from patient-derived induced pluripotent stem cells showed arrest at the myeloid progenitor stage and apoptotic predisposition, both of which replicated abnormal granulopoiesis. Moreover, lentiviral transduction of the *HAX1* cDNA into patient-derived induced pluripotent stem cells reversed disease-related abnormal granulopoiesis. This *in vitro* neutrophil differentiation system, which uses patient-derived induced pluripotent stem cells for disease investigation, may serve as a novel experimental model and a platform for high-throughput screening of drugs for various congenital neutrophil disorders in the future.

Introduction

Severe congenital neutropenia (SCN) is a rare myelopoietic disorder resulting in recurrent life-threatening infections due to a lack of mature neutrophils,[1] and individuals with SCN present for myeloid hypoplasia with an arrest of myelopoiesis at the promyelocyte/myelocyte stage.[1,2] SCN is actually a multigene syndrome that can be caused by inherited mutations in several genes. For instance, approximately 60% of SCN patients are known to carry autosomal dominant mutations in the *ELANE* gene, which encodes neutrophil elastase (NE).[3] An autosomal recessive type of SCN was first described by Kostmann in 1956,[4] and defined as Kostmann disease. Although the gene responsible for this classical type of SCN remained unknown for more than 50 years, Klein *et al.* identified mutations in *HAX1* to be responsible for this type of SCN in 2007.[5] HAX1 localizes predominantly to mitochondria, where it controls inner mitochondrial membrane potential ($\Delta\psi_m$) and apoptosis.[6,7] Although an increase in apoptosis in mature neutrophils was presumed to cause neutropenia in HAX1 gene deficiency,[5] the connection between *HAX1* gene mutations and defective granulopoiesis in SCN has remained unclear.

To control infections, SCN patients are generally treated with granulocyte colony-stimulating factor (G-CSF); however, long-term G-CSF therapy associates with an increased risk of myelodysplastic syndrome and acute myeloid leukemia (MDS/AML).[8,9] Although hematopoietic stem cell transplantations are available as the only curative therapy for this disease, they can result in various complications and mortality.[4]

Many murine models of human congenital and acquired diseases are invaluable for disease investigation as well as for novel drug discoveries. However, their use in a research setting can be limited if they fail to mimic strictly the phenotype of the human disease in question. For instance, the *Hax1* knock-out mouse is characterized by lymphocyte loss and neuronal apoptosis, but not neutropenia.[10] Thus, it is not a suitable experimental model for SCN. Induced pluripotent stem (iPS) cells are reprogrammed somatic cells with embryonic stem (ES) cell-like characteristics produced by the introduction of specific transcription factors,[11,16] and they may substitute murine models of human disease. It is believed that iPS cell technology, which generates disease-specific pluripotent stem cells in combination with directed cell differentiation, will contribute enormously to patient-oriented research, including disease pathophysiology, drug screening, cell transplantation, and gene therapy.

In vitro neutrophil differentiation systems, which can reproduce the differentiation of myeloid progenitor cells to mature neutrophils, are needed to understand the pathogenesis of SCN better. Recently, we established a neutrophil differentia-

 doi:10.3324/haematol.2013.083873
The online version of this article has a Supplementary Appendix.
Manuscript received on January 9, 2013. Manuscript accepted on August 20, 2013.
Correspondence: heike@kuhp.kyoto-u.ac.jp

tion system from human iPS cells[17] as well as a serum- and feeder-free monolayer hematopoietic culture system from human ES and iPS cells.[18] In this study, we generate iPS cell lines from an SCN patient with *HAX1* gene deficiency and differentiate them into neutrophils *in vitro*. Furthermore, we corrected for the *HAX1* gene deficiency in HAX1-iPS cells by lentiviral transduction with *HAX1* cDNA and analyzed the neutrophil differentiation potential of these cells. Thus, this *in vitro* neutrophil differentiation system from patient-derived iPS cells may be a useful model for future studies in SCN patients with *HAX1* gene deficiency.

Methods

Human iPS cell generation

Skin biopsy specimens were obtained from an 11-year old male SCN patient with *HAX1* gene deficiency.[19] This study was approved by the Ethics Committee of Kyoto University, and informed consent was obtained from the patient's guardians in accordance with the Declaration of Helsinki. Fibroblasts were expanded in DMEM (Nacalai Tesque, Inc., Kyoto, Japan) containing 10% FBS (vol/vol, Invitrogen, Carlsbad, CA, USA) and 0.5% penicillin and streptomycin (wt/vol, Invitrogen). Generation of iPS cells was performed as described previously.[12] In brief, we introduced *OCT3/4, SOX2, KLF4*, and *cMYC* using ecotropic retroviral transduction into patient's fibroblasts expressing mouse *Slc7a1*. Six days after transduction, cells were harvested and re-plated onto mitotically inactive SNL feeder cells. On the following day, DMEM was replaced with primate ES cell medium (ReproCELL, Kanagawa, Japan) supplemented with basic fibroblast growth factor (5 ng/mL, R&D Systems, Minneapolis, MN, USA). Three weeks later, individual colonies were isolated and expanded.

Maintenance of cells

Control ES (KhES-1) and control iPS (253G4 and 201B6) cells were kindly provided by Drs. Norio Nakatsuji and Shinya Yamanaka (Kyoto University, Kyoto, Japan), respectively. These human ES and iPS cell lines were maintained on mitomycin-C (Kyowa Hakko Kirin, Tokyo, Japan)-treated SNL feeder cells as described previously[17] and subcultured onto new SNL feeder cells every seven days.

Flow cytometric analysis

Cells were stained with antibodies as reported previously.[17] Samples were analyzed using an LSR flow cytometer and Cell Quest software (Becton-Dickinson).

Neutrophil differentiation of iPS cells

In a previous study, we established a serum and feeder-free monolayer hematopoietic culture system from human ES and iPS cells.[18] In this study, we modified this culture system to direct neutrophil differentiation. iPS cell colonies were cultured on growth factor-reduced Matrigel (Becton-Dickinson)-coated cell culture dishes in Stemline II hematopoietic stem cell expansion medium (Sigma-Aldrich, St. Louis, MO, USA) containing the insulin-transferrin-selenium (ITS) supplement (Invitrogen) and cytokines. iPS cells were treated with cytokines as follows: bone morphogenetic protein (BMP) 4 (20 ng/mL, R&D Systems) was added for four days and then replaced with vascular endothelial growth factor (VEGF) 165 (40 ng/mL, R&D Systems) on Day 4. On Day 6, VEGF 165 was replaced with a combination of stem cell factor (SCF, 50 ng/mL, R&D Systems), interleukin (IL)-3 (50 ng/mL, R&D Systems), thrombopoietin (TPO, 5 ng/mL, kindly provided by Kyowa Hakko Kirin), and G-CSF (50 ng/mL, also kindly provided by Kyowa Hakko Kirin). Thereafter, medium was replaced every five days.

Dead cell removal and CD45$^+$ leukocyte separation

Floating cells were collected, followed by the removal of dead cells and cellular debris with the Dead Cell Removal kit (Miltenyi Biotec, Bergisch Gladbach, Germany). CD45$^+$ cells were then separated using human CD45 microbeads (Miltenyi Biotec). Cell separation procedures were performed using the autoMACS Pro Separator (Miltenyi Biotec).

Statistical analysis

Statistical analysis was carried out using Student's t-test. $P<0.05$ was considered statistically significant.

Results

Generation of iPS cell lines from an SCN patient with HAX1 gene deficiency

To generate patient-derived iPS cell lines, dermal fibroblasts were obtained from a male SCN patient with a homozygous 256C-to-T transition resulting in an R86X mutation in the *HAX1* gene.[19] These fibroblasts were reprogrammed to iPS cells after transduction with retroviral vectors encoding *OCT3/4, SOX2, KLF4* and *cMYC*,[12] and a total of 11 iPS cell clones were obtained. From these, we randomly selected three clones for propagation and subsequent analyses. One of these clones (HAX1 4F5) was generated with four factors (*OCT3/4, SOX2, KLF4*, and *cMYC*); the remaining clones (HAX1 3F3 and 3F5) were generated with three factors (*OCT3/4, SOX2*, and *KLF4*).[12]

All of these patient-derived iPS cell clones showed a characteristic human ES cell-like morphology (Figure 1A), and they propagated for serial passages in human ES cell maintenance culture medium. Quantitative PCR analysis showed the expression of *NANOG*, a pluripotent marker gene, to be comparable to that of control ES (KhES-1) and iPS (253G4 and 201B6) cells (Figure 1B). Surface marker analysis indicated that they were also positive for SSEA4, a human ES and iPS cell marker (Figure 1C). DNA sequencing analysis verified an identical mutation in the *HAX1* gene in all established iPS cell clones (Figure 1D). The pluripotency of all iPS cell clones was confirmed by the presence of cell derivatives representing all three germ layers by teratoma formation after subcutaneous injection of undifferentiated iPS cells into immunocompromised NOD/SCID/γc^{null} mice (Figure 1E).

To validate the authenticity of iPS cells further, we investigated the expression of the four genes that were used for iPS cell generation. The expression level of all endogenous genes was comparable to control ES and iPS cells. On the other hand, transgene expression was largely undetectable in patient-derived iPS cell clones (*Online Supplementary Figure S1A*). Chromosomal analysis revealed that all patient-derived iPS cell clones maintained a normal karyotype (*Online Supplementary Figure S1B*). Genetic identity was shown by short tandem repeat analysis (*Online Supplementary Figure S1C*).

Taken collectively, these results indicate that iPS cell clones were comprised of good quality iPS cells derived from the somatic cells of an SCN patient with *HAX1* gene deficiency (HAX1-iPS cells).

Maturation arrest at the progenitor level in neutrophil differentiation from HAX1-iPS cells

The paucity of mature neutrophils in the peripheral blood and a maturation arrest at the promyelocyte/myelocyte stage in the bone marrow are characteristic laboratory findings presented in the SCN patients with *HAX1* gene deficiency. To investigate whether our patient-derived iPS cell model accurately replicated this disease phenotype, we assessed neutrophil differentiation from HAX1-iPS cells by using a serum- and feeder-free monolayer culture system[18] with minor modifications (Online *Supplementary Figure S2*).

In this system, we cultured iPS cell colonies on Matrigel-coated dishes in serum-free medium supplemented with several cytokines and obtained hematopoietic cells as floating cells on approximately Day 26 of differentiation. May-Giemsa staining of floating live $CD45^+$ cells derived from normal iPS cells showed that approximately 40% were mature neutrophils (Figure 2A and B). The remaining cells consisted of immature myeloid cells as well as a small number of macrophages. Cells of other lineages such as erythroid or lymphoid cells were not observed. On the other hand, HAX1-iPS cell-derived blood cells contained only approximately 10% mature neutrophils and approxi-

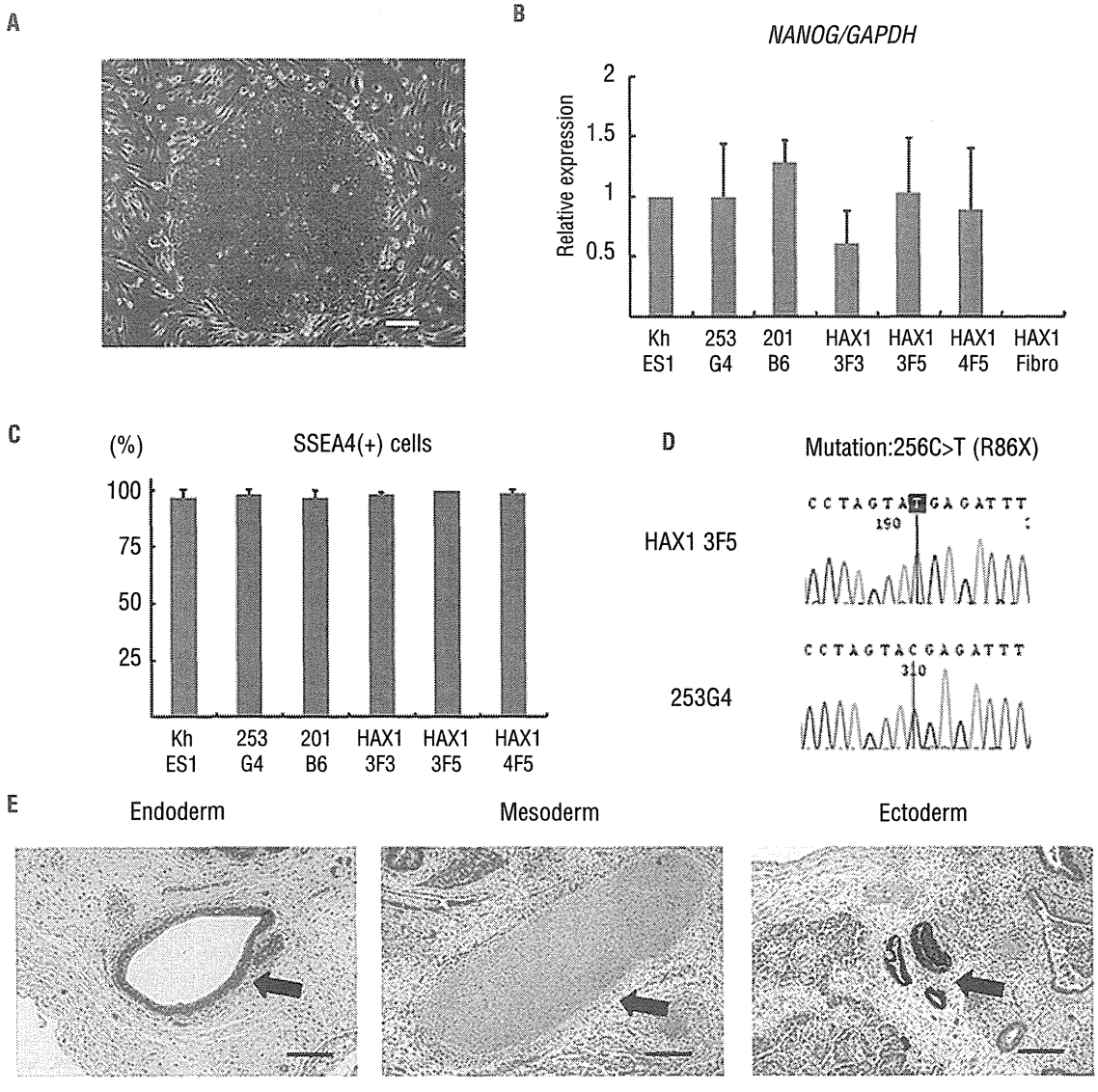

Figure 1. **Generation of iPS cell lines from an SCN patient with *HAX1* gene deficiency.** (A) Human ES cell-like morphology of HAX1-iPS cells. Scale bar: 200 μm. (B) *NANOG* expression in HAX1-iPS cells, control iPS cells (253G4 and 201B6), and patient-derived fibroblasts (HAX1 Fibro) compared to control ES cells (KhES1). *GAPDH* was used as an internal control (n = 3; bars represent SDs). (C) SSEA-4 expression analysis using flow cytometry. Gated on $TRA1\text{-}85^+DAPI^-$ cells as viable human iPS (ES) cells (n = 3; bars represent SDs). (D) DNA sequencing analysis of the *HAX1* gene in iPS cells. HAX1-iPS cells showed 256C>T (R86X) mutation that was found in the patient. (E) Teratoma formation from HAX1-iPS cells in the NOD/SCID/γc^{null} (NOG) mouse. Arrows indicate the following; Endoderm: respiratory epithelium; Mesoderm: cartilage; Ectoderm: pigmented epithelium. Scale bars: 200 μm. (A, D-E) Representative data (HAX1 3F5) are shown.

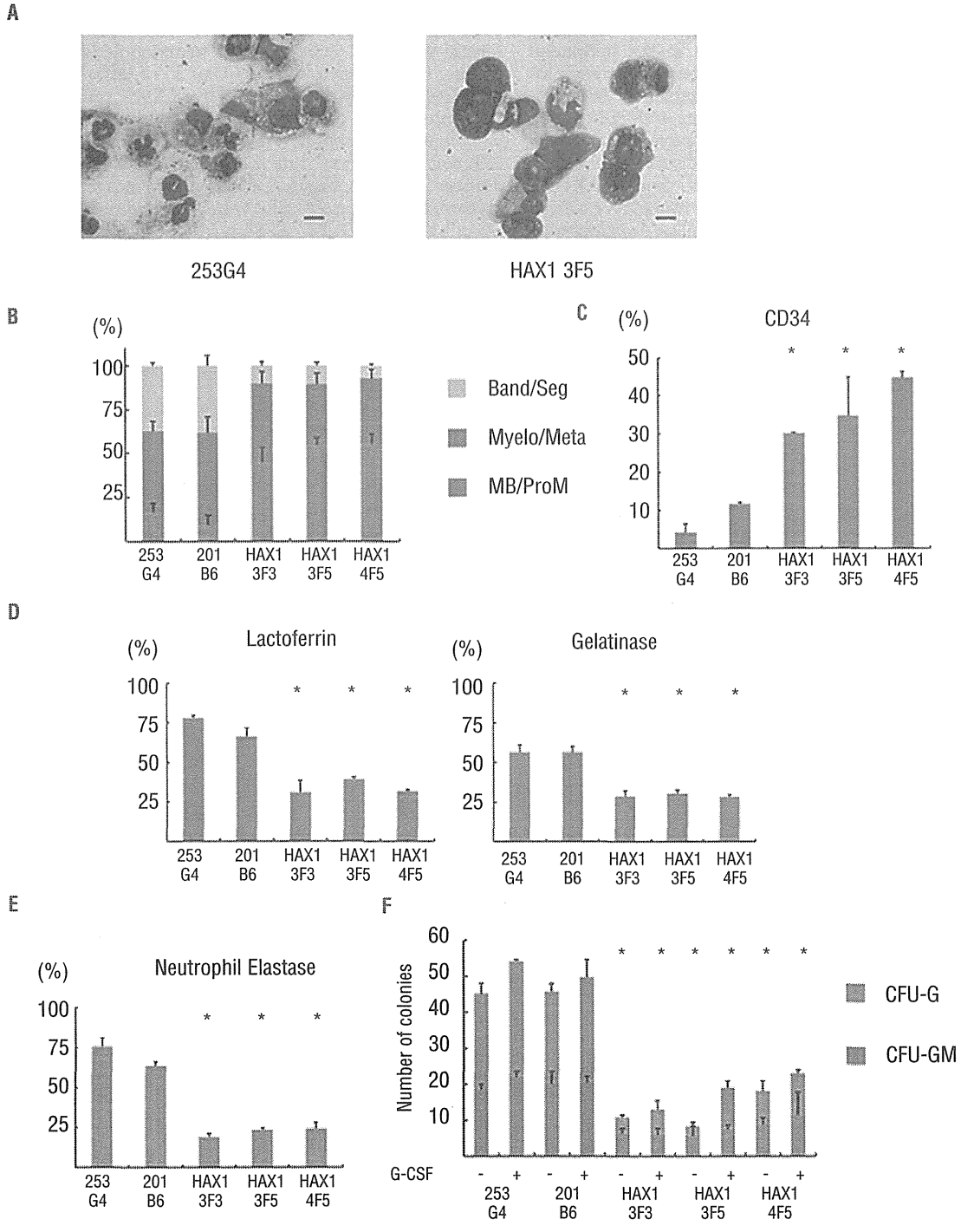

Figure 2. Maturation arrest at the progenitor level in neutrophil differentiation from HAX1-iPS cells. (A) May-Giemsa staining of CD45$^+$ cells derived from normal (253G4) and HAX1-iPS (HAX1 3F5) cells. Scale bars: 10 μm. (B) Morphological classification of CD45$^+$ cells derived from iPS cells. Cells were classified into three groups: myeloblast and promyelocyte (MB/ProM), myelocyte and metamyelocyte (Myelo/Meta), and band and segmented neutrophils (Band/Seg) (n = 3; bars represent SDs). (C) Flow cytometric analysis of CD45$^+$ cells derived from iPS cells. Cells gated on human CD45$^+$ DAPI$^-$ were analyzed (n = 3; bars represent SDs; *P<0.05 compared to control iPS cells). (D) Immunocytochemical analysis of CD45$^+$ cells derived from iPS cells (n = 3; bars represent SDs; *P<0.05 compared to control iPS cells). (E) NE staining of CD45$^+$ cells derived from iPS cells (n = 3; bars represent SDs; *P<0.05 compared to control iPS cells). (F) Colony-forming assay of cells derived from iPS cells. On Day 16, living adherent cells were collected and cultured in methylcellulose medium (see *Online Supplementary Appendix*). The number of colonies generated from 1×10^4 cells is indicated (n = 3; bars represent SD; *P<0.05 compared to control iPS cells). (A–E) Live CD45$^+$ cells derived from normal and HAX1-iPS cells on Day 26 of neutrophil differentiation were analyzed. Dead cells and CD45$^-$ cells were depleted using an autoMACS Pro separator (see *Methods*).

mately 50% immature myeloid cells, including myeloblasts and promyelocytes (Figure 2A and B). Flow cytometric analysis revealed that the percentage of CD34$^+$ cells within HAX1-iPS cell-derived blood cells was significantly higher than in normal iPS cell-derived blood cells (Figure 2C), which also showed that the percentage of phenotypically immature myeloid cells was higher in HAX1-iPS cell-derived blood cells than in normal iPS cell-derived blood cells.

Immunocytochemical analysis for lactoferrin and gelatinase, which are constitutive proteins of neutrophil specific granules observed in mature neutrophils, showed that the proportion of these granule-positive cells was significantly lower in HAX1-iPS cell-derived blood cells than in normal iPS cell-derived blood cells (Figure 2D). NE is a protease stored in primary granules of neutrophilic granulocytes that are formed at the promyelocytic phase of granulocyte differentiation. *ELANE* mRNA expression in myeloid progenitors and the protein level of NE in plasma are markedly reduced in SCN patients with mutations in *ELANE* or *HAX1*.[20] Consistent with this, the proportion of NE-positive cells was significantly lower in blood cells derived from HAX1-iPS cells than in those derived from normal iPS cells (Figure 2E). Thus, the level of functionally mature neutrophils decreased during *in vitro* granulopoietic differentiation of HAX1-iPS cells.

Next, we analyzed the colony-forming potential of HAX1-iPS cell-derived myeloprogenitor cells. Significantly fewer colonies, which were classified as granulocyte-macrophage (GM) or granulocyte (G) colony-forming units (CFU), were derived from HAX1-iPS cells than from control iPS cells. Furthermore, the colonies derived from HAX1-iPS cells were predominantly CFU-GM (Figure 2F). Thus, maturation arrest occurred at the clonogenic progenitor stage during *in vitro* neutrophil differentiation of HAX1-iPS cells.

SCN is characterized by severe neutropenia with very low absolute neutrophil counts in peripheral blood, and many SCN patients respond to G-CSF treatment.[1,2] In colony-forming assays using bone marrow cells of SCN patients, primitive myeloid progenitor cells have reduced responsiveness to hematopoietic cytokines including G-CSF.[21,22] Therefore, we next examined the response of HAX1-iPS cell-derived blood cells to G-CSF using a colony-forming assay. Although the number of colonies derived from HAX1-iPS cells slightly increased following the addition of G-CSF, it remained significantly lower than the number of colonies derived from control iPS cells in the absence of G-CSF (Figure 2F). These results indicate that the responsiveness of HAX1-iPS-derived blood cells to G-CSF was insufficient to restore the neutrophil count to a normal level and are consistent with the fact that the absolute neutrophil counts of SCN patients remain low following G-CSF therapy.[19,21]

Neutrophils derived from HAX1-iPS cells are predisposed to undergo apoptosis due to their reduced $\Delta\psi_m$

Previous studies have shown HAX1 to localize to mitochondria[6] and to mediate anti-apoptotic activity.[7] Interestingly, this apoptotic predisposition of neutrophils due to their reduced $\Delta\psi_m$ was observed in HAX1-deficient patients,[5] prompting us to examine apoptosis in HAX1-iPS cell-derived blood cells. Consistent with these reports, HAX1-iPS cell-derived blood cells showed a significantly higher percentage of Annexin V-positive cells than in control cells (Figure 3A). In addition, a mitochondrial membrane potential assay revealed that the percentage of cells with a low $\Delta\psi_m$ was significantly higher in HAX1-iPS cell-derived blood cells than in blood cells derived from control iPS cells (Figure 3B). By contrast, the percentage of cells with a low $\Delta\psi_m$ was similar in undifferentiated HAX1-iPS cells and undifferentiated control iPS cells (*Online Supplementary Figure S3*).

Thus, increased apoptosis due to reduced $\Delta\psi_m$ causes defective granulopoiesis during neutrophil differentiation from HAX1-iPS cells, similar to the process observed in SCN patients with *HAX1* gene deficiency.

Lentiviral transduction of HAX1 cDNA improves maturation arrest and apoptotic predisposition of HAX1-iPS cells

Because most *HAX1* gene mutations in SCN patients are nonsense mutations resulting in a premature stop codon and protein truncation,[23] loss of the HAX1 protein is believed to cause severe neutropenia. To uncover the pathophysiological hallmarks of this disease, we performed lentiviral transduction of *HAX1* cDNA into HAX1-iPS cells.

We constructed lentiviral vectors that expressed *HAX1* cDNA and EGFP as a marker gene (pCSII-EF-IEGFP; EGFP

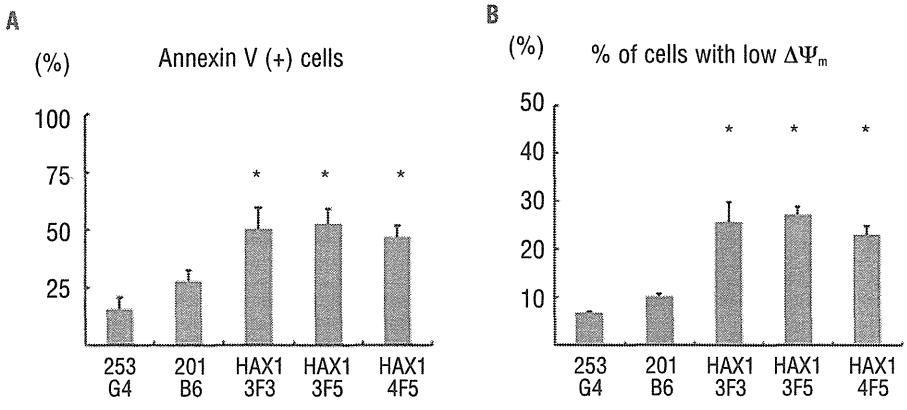

Figure 3. **Neutrophils derived from HAX1-iPS cells are predisposed to undergo apoptosis due to their reduced $\Delta\psi$m. Annexin V assay (A) and mitochondrial membrane potential assay (B) of iPS cell-derived cells on Day 26 of neutrophil differentiation using flow cytometry. Cells gated on human CD45$^+$ were analyzed (n = 3; bars represent SDs; *P<0.05 to control iPS cells).**

only, pCSII-EF-HAX1-IEGFP; HAX1 cDNA and EGFP) (Figure 4A). Efficient transduction of HAX1-iPS cells with these lentiviral vectors (HAX1 3F5+GFP; HAX1 3F5 transduced with pCSII-EF-IEGFP, HAX1 3F5+HAX1; HAX1 3F5 transduced with pCSII-EF-HAX1-IEGFP) was confirmed by a significant increase in HAX1 protein by Western blotting analysis (Figure 4B).

We then differentiated these lentiviral-transduced iPS cells into neutrophils, and examined whether defective granulopoiesis and apoptotic predisposition could be reversed. Morphologically, cells derived from HAX1 3F5+HAX1 showed a higher proportion of mature neutrophils than cells derived from HAX1 3F5+GFP and HAX1 3F5 (Figure 5A and B). Flow cytometric analysis revealed that the proportion of $CD34^+$ cells was significantly lower in the cells derived from HAX1 3F5+HAX1 than HAX1 3F5+GFP and HAX1 3F5 (Figure 5C). Immunocytochemical analysis for lactoferrin and gelatinase showed that the proportion of these granule-positive cells in generated blood cells was significantly higher in HAX 3F5+HAX1 than in HAX13F5+GFP and HAX1 3F5 (Figure 5D). These results indicated that *HAX1* cDNA increased the number of mature neutrophils in the neutrophil differentiation culture from HAX1-iPS cells *in vitro*. In addition, the percentage of NE-positive cells was significantly higher in cells derived from HAX1 3F5+HAX1 than in cells derived from HAX1 3F5+GFP and HAX1 3F5 (Figure 5E). Furthermore, the number of colonies derived from HAX1 3F5+HAX1 was comparable to the number derived from control cells (Figure 5F).

HAX1 3F5+HAX1-derived blood cells showed a significantly lower percentage of Annexin V-positive cells (Figure 6A) and a significantly lower percentage of cells with a low $\Delta\psi_m$ (Figure 6B) than HAX13F5+GFP and HAX1 3F5-derived blood cells. These results indicated that only *HAX1* cDNA transduction improved defective granulopoiesis and apoptotic predisposition due to low $\Delta\psi_m$ in the neutrophil differentiation culture from HAX1-iPS cells *in vitro*.

Discussion

Animal models and *in vitro* cultures consisting of cells derived from patients are often used to investigate disease pathophysiology and to develop novel therapies. Unfortunately, *Hax1* knock-out mice fail to reproduce abnormal granulopoiesis as observed in SCN patients.[10] Moreover, bone marrow cells are not an ideal experimental tool because it is difficult to obtain sufficient blood cells due to the invasiveness of the aspiration procedure. Moreover, the pathophysiological mechanisms occurring during early granulopoiesis are difficult to address in primary patient samples.

Our established culture system efficiently induced directed hematopoietic differentiation, which consisted of myeloid cells at different stages of development, from various control and patient-derived HAX1-iPS cell lines. Furthermore, this *in vitro* neutrophil differentiation system produced sufficient myeloid cells, which enabled us to perform various types of assays. In addition, flow cytom-

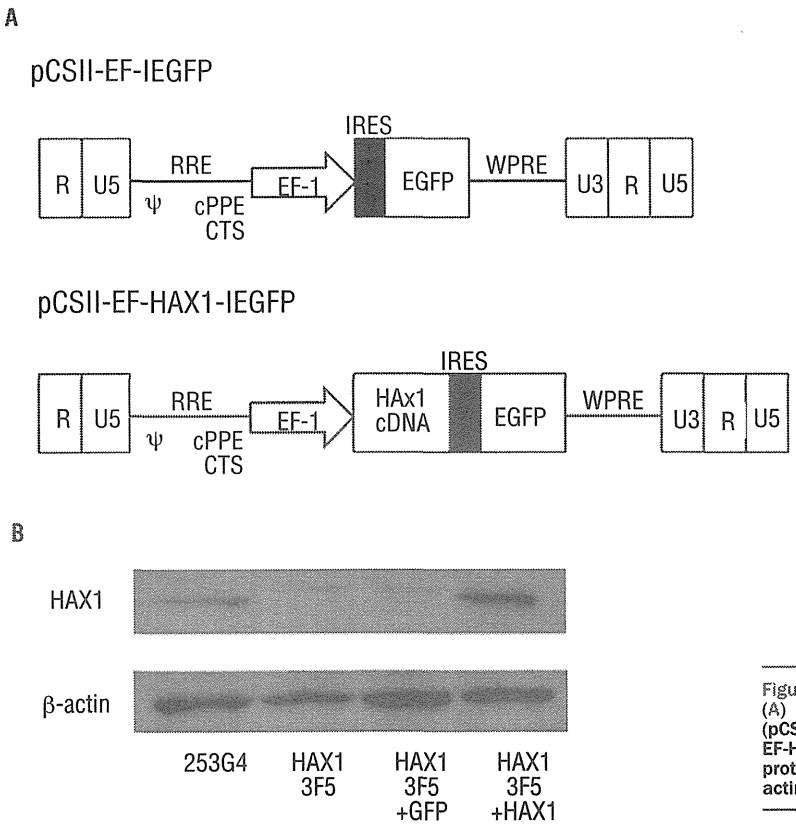

Figure 4. **Lentiviral transduction of HAX1-iPS cells. (A) Lentiviral vector constructs with only EGFP (pCSII-EF-IEGFP), and *HAX1* cDNA and EGFP (pCSII-EF-HAX1-IEGFP). (B) Western blot analysis for HAX1 protein in lentivirally-transduced HAX1-iPS cells. β-actin was used as a loading control.**

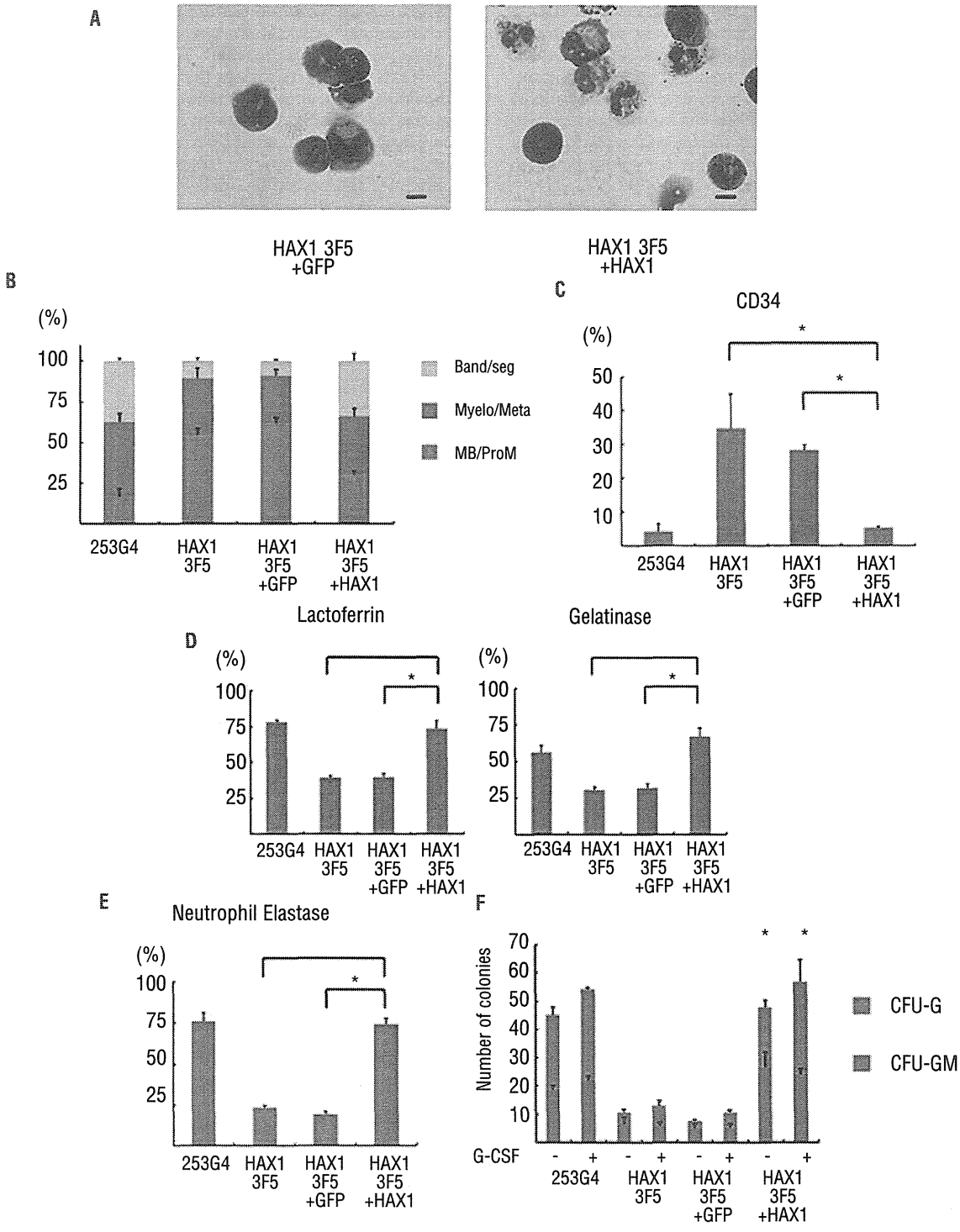

Figure 5. **Lentiviral transduction of HAX1 cDNA improves maturation arrest of HAX1-iPS cells.** (A) May-Giemsa staining of CD45$^+$ cells derived from HAX1 3F5+GFP and HAX1 3F5+HAX1 cells. Scale bars: 10 μm. (B) Morphological classification of CD45$^+$ cells derived from lentivirally-transduced iPS cells. (n = 3; bars represent SDs). (C) Flow cytometric analysis of CD45$^+$ cells derived from lentivirally-transduced iPS cells. Cells gated on GFP$^+$ human CD45$^+$ DAPI$^-$ were analyzed (n = 3; bars represent SDs; *P<0.05). (D) Immunocytochemical analysis of CD45$^+$ cells derived from lentivirally-transduced iPS cells (n = 3; bars represent SDs; *P<0.05). (E) NE staining of CD45$^+$ cells derived from lentivirally-transduced iPS cells (n = 3; bars represent SDs; *P<0.05). (F) Colony-forming assay of lentivirally-transduced cells derived from iPS cells. The number of colonies derived from 1×10^4 cells is indicated (n = 3; bars represent SD; *P<0.05 compared to HAX1 3F5 and HAX1 3F5+GFP). (A-E) Live CD45$^+$ cells derived from lentivirally-transduced iPS cells on Day 26 of neutrophil differentiation were analyzed. Dead cells and CD45$^-$ cells were depleted using an autoMACS Pro separator (see *Methods*).